A NOVEL PATHOLOGY DEVICE FOR THE IMPROVEMENT OF INTRAOPERATIVE BREAST CANCER TISSUE GROSS EXAMINATION

By

Xenia Kachur

A Thesis Submitted to the Faculty of the

BIOMEDICAL ENGINEERING GRADUATE INTERDISCIPLINARY PROGRAM

In Partial Fulfillment of the Requirements

For the Degree of

MASTER OF SCIENCE

In the Graduate College

THE UNIVERSITY OF ARIZONA

2011

APPROVAL BY THESIS DIRECTOR

This thesis has been approved on the date shown below:

A. Arabyan

Ara Arabyan, Ph.D.

Associate Professor of Aerospace
and Mechanical Engineering

December 6, 2011

Date

ACKNOWLEDGEMENT

I would like to thank several people for their help and support during the period that it has taken me to complete this degree. First, I'd like to thank my mentor, Dr. Ara Arabyan, for trusting in my abilities and facilitating the development of this project. I would also like to thank Dr. Don Uhlmann for his continued support and tremendous insight throughout my time in the program.

Additionally, I would like to thank the people who aided in the experimentation and analysis of the collected data. The gel setting and temperature experiments were conducted at a private laboratory, located at 3496 S. Dodge Blvd, with the help of laboratory technicians Kyle Troyer and Steven Banister. The X-ray attenuation data was collected at the Cancer Imaging Shared Service laboratory in the Arizona Cancer Center with the assistance of laboratory technician Justin Jeffery and Dr. Natarajan Raghunand. The first part of the gel-tissue interaction study was conducted at the Southern Arizona Veterinary Specialty and Emergency center with tissue being supplied by Drs. Mary Kay Klein and Jennifer Wendt. The processing of the tissue was conducted at the Arizona Veterinary Diagnostic Laboratory where Dr. Sharon Dial performed the tissue microanalysis.

Lastly, I would like to thank my wonderful partner, Alex, who is relentlessly supportive in every aspect of my life and helps keep me focused on what is truly important.

TABLE OF CONTENTS

LIST OF FIGURES

LIST OF TABLES

ABSTRACT

The aim of this study was to design and test key aspects of a novel device, consisting of a polymer referencing enclosure (hardware) and a gel component, for the standardization of intraoperative gross pathology examination of excised breast cancer tissue. The proposed device improves the current practice of tissue preparation for radiographic and pathological examination without changing the existing process and without imposing retraining requirements on professional staff involved in the current process. To identify the optimal composition of the gel component to be used, 32 gel formulations were tested to determine setting times and maximum temperature reached during setting. The radiographic properties of 12 gel formulations and 15 plastic materials for potential use in the hardware were also tested. A negative correlation was found to exist between setting time and maximum temperature reached, narrowing down gel selections to those setting in <10 minutes with a temperature peak of <54°C. The radiographic properties of the tested and downselected gels and plastics were found to be such that these materials are unlikely to interfere with lesion identification in radiological examinations. A completed tissue study for examination of gel effects on tissue properties revealed no effects, thereby clearing this device for potential clinical applications.

I. CURRENT PROCEDURES USED IN TUMOR SPECIMEN PREPARATION

In this section, we will begin with an overview of breast cancer progression, causes, and prevalence. Then, we will describe breast cancer treatment options, current technologies and practices used in treatments, and the subsequent limitations of these practices. This will provide a foundation for outlining our novel device solution and the affiliated studies that we performed.

A. What is breast cancer and what is its cause?

Breast cancer is a malignant group of cells located in the breast tissue that proliferates uncontrollably and has the potential to metastasize to other areas of the body (American Cancer Society, 2011). It is a disease that most prominently occurs in women due to the structure and functions of the tissues in the breast and affects over 4.3 million people worldwide (SEER, 2008). Figure I.1 below illustrates the normal structure of a female breast.

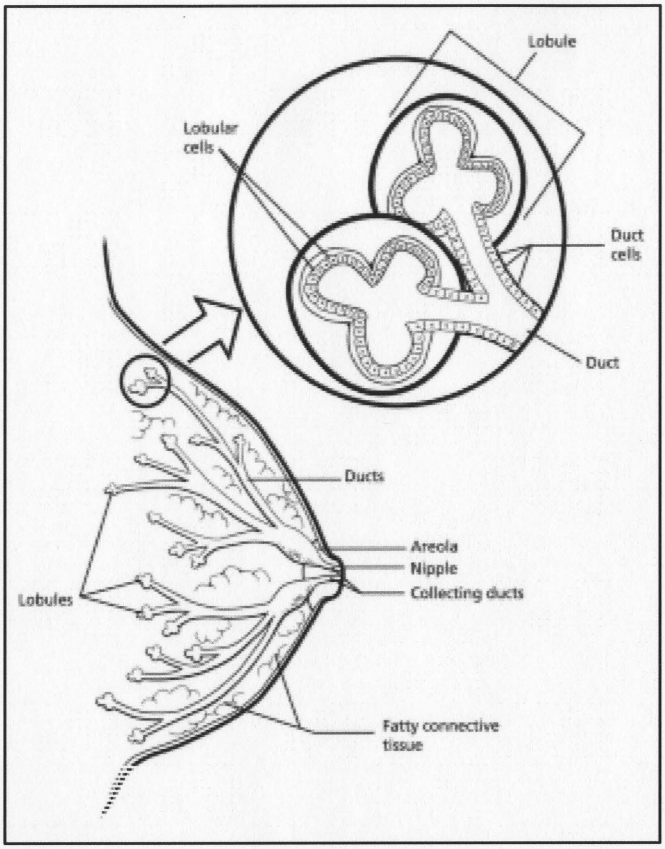

Figure I.1. Anatomy of the female breast (AMERICAN CANCER SOCIETY, 2011).

Breast cancers are classified based on the characteristics of tissue of origin, invasiveness and disease progression. The majority of breast cancers begin in the milk ducts, responsible for carrying milk from the production sites, or lobules, to the nipple. In all forms of breast cancer, invasiveness is of high concern due to the proximity of the lymphatic system, the network of vessels through which lymph drains from the tissues into the blood, to the breast tissue. If the cancer spreads to the lymph nodes, the risk of metastasis is increased significantly because the lymphatic system facilitates transfer of cancerous cells to other areas of the body through the blood (American Cancer Society, 2011).

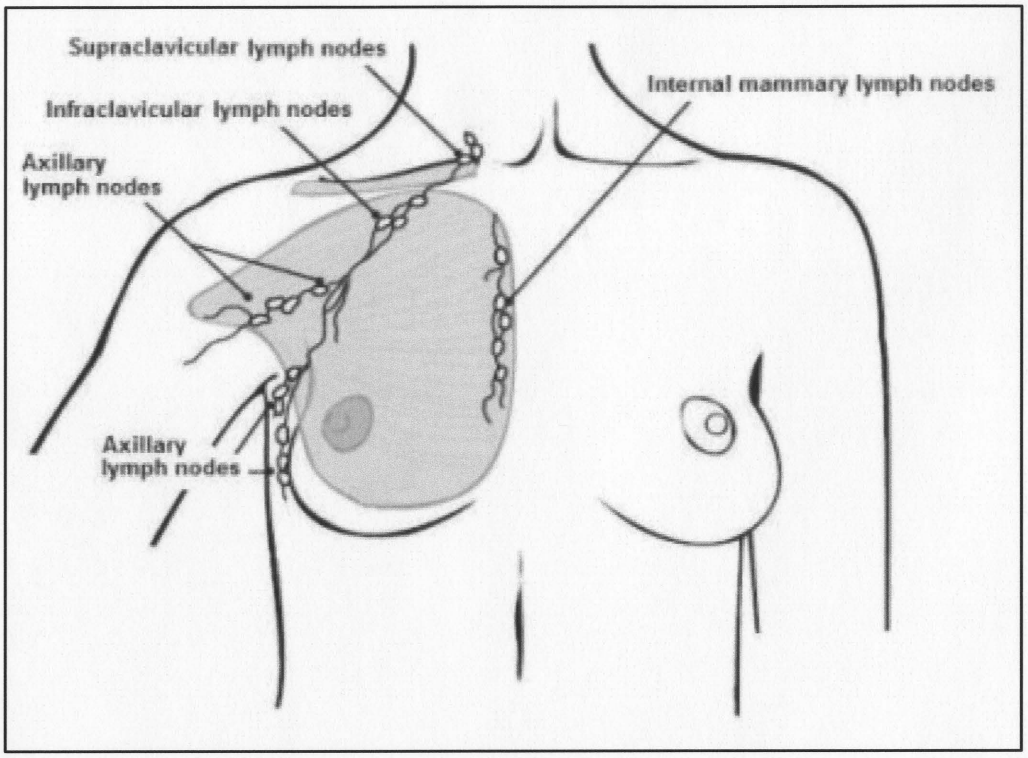

Figure I.2. Structure and organization of the lymphatic system in the breast tissue (AMERICAN CANCER SOCIETY, 2011).

Like the majority of cancers, there is no known definitive cause of breast cancer. Despite this, increased risk of breast cancer has been associated with the following: hormone replacement therapy (Rossouw JE, 2002), up-regulation of HER2 gene expression (Tzu-Chao, 2011) and overexpression of IGF-I or IGF-I receptors (Kleinberg, 2009), toxins such as atrazine (Simpkins, 2011), reproductive history (Russo, 2011), and germline mutations in genes such as BRCA1 and BRCA2 (Hughes, 2008).

Regardless of the predicted causes of disease progression, early detection is pertinent to survival and recovery. The most common methods of detecting the formation of breast tumors are through palpation, or manual breast examination, and radiographic screening. In both of these processes, the screener attempts to locate a hard lump with the

fingers in examination or a dense mass using mammography; the look and feel of the tumor is often the result of microcalcifications, or characteristic clusters of calcium deposits. The formation of microcalcifications is most often due to one or more of the following: cysts in the breast tissue, cell secretions or debris, ductal carcinoma in situ, fibroadenoma, mammary duct ectasia, mastitis, or dermal vascular calcification (Mayo Clinic, 2011). However, not all breast cancers have high-contrast microcalcifications present.

Early manifestations of breast cancer can be very subtle and are identified as a complex and variable pattern in contrast to normal anatomy (Vyborny, 2000). Early detection is heavily reliant on the radiologist's ability to identify characteristic lesions, sometimes at very low contrast to the surrounding tissue (Ishida, 1996). In order to increase the reliability of diagnosis, imaging modalities and computerized detection software are being improved and developed (Alexander, 2011) (Yuan-Zhi, 2011) (Felix, 2011) (Dorrius, 2011) (Schmidt, 2011) (Vyborny, 2000).

B. Treatment Approaches

Surgical procedures

When a tumor is suspected to be present on a radiograph, a sample of breast tissue cells in the area of the suspicious mass is taken in a process called fine needle aspiration biopsy. To conduct this biopsy, a hollow needle is used to extract cells from the suspicious area of tissue, and then the fluid cell sample is tested and analyzed by a

pathologist to determine the extent of malignancy. Surgical intervention is the most common first form of treatment when malignancy is found.

Surgery is sometimes coupled with additional treatments such as radiation (Croshaw, 2011), chemotherapy (Kurbet, 2006), or thermal ablation (Zhao, 2010). Generally, the patient is must decide, with the physician's guidance, between modified radical mastectomy, the surgical removal of the all breast tissue and lymph nodes, or a lumpectomy, the removal of only the diseased tissue with a narrow rim of healthy tissue surrounding it.

Studies comparing the long-term results of radical mastectomy as compared to lumpectomy procedures have shown that there is no significant difference in overall survival between the two groups (Fisher B. B., 1985) (Fisher B. A., 1995) (Fisher B. A., 2002). However, they also found that women undergoing lumpectomy with breast irradiation had statistically decreased incidence rates of recurrence in the ipsilateral breast as compared to lumpectomy alone (Fisher B. A., 2002). Some argue that a wider margin of healthy breast tissue surrounding the excised tumor would diminish this difference (Silverstein, 1999).

Despite these encouraging statistics, with over 200,000 new cases of breast cancer diagnosed every year, half of patients eligible for lumpectomy still choose mastectomy. This is likely to be due to a one or more reasons including the following: physicians educated before the 1980s are more familiar with the procedures and results of mastectomies, insurance coverage of lumpectomies is not always available, socio-economic factors, age of the patient, and the psychological well-being of feeling "safer"

against potential cancer recurrence (The Breast Care Site, 2011). Another major factor that affects patients' decisions is the incidence of repeat surgery following breast-conserving surgery. Approximately one in three patients that choose breast-conserving procedures, such as lumpectomy, must have repeat surgery within weeks, sometimes resulting in up to four re-excision surgeries or a conversion to mastectomy (Brown, 2010) (Guenther, 1996) (Uecker, 2011). Furthermore, procedures lacking intraoperative assessment of tumor margins result in 60% likelihood that a patient has to return for a repeat surgical excision procedure (Uecker, 2011). These staggering statistics mean that tens of thousands of women each year return for multiple unnecessary high risk surgeries, a number that we aim to reduce.

Our goal with this device is to provide a means by which pathologists can more accurately and easily assess tumor margins intraoperatively for the purpose of decreasing the incidence rate of repeat surgery and local recurrence and make breast-conserving surgery a viable option for more women.

Pathology tumor margin analysis process & limitations

Once the cancerous tissue is excised from a patient as part of the surgical treatment process, steps are taken to ensure that the entirety of the diseased tissue has been removed and to guide subsequent treatment protocols. The method by which complete removal of the tumor is determined is by analyzing whether there is cancer present near the margins of the excised tissue specimen; if there is cancerous tissue within 2 mm of the edge of the tissue, it is identified as a 'positive margin'. This indicates that there is a high likelihood that part of the tumor was left behind in the breast. The

initial step in this tissue assessment process is called gross pathologic examination. In certain surgical procedures, gross examination is performed while the patient is still on the operating table and is referred to as intraoperative tissue assessment. In breast-conserving surgery, intraoperative gross pathologic examination of excised breast tissue is designed to assist the surgeon in identifying any cancerous tissue not removed from the patient, while simultaneously aiming to retain as much healthy tissue as possible.

Once the tumor has been excised, the surgeon orients the specimen as it was in the body using either orientation clips or sutures that correspond to directions in the body. For example, a long suture is placed on the tissue side that corresponds to the lateral side of the body, a short suture is placed on the superior side, and a medium length suture is placed on the medial side. The purpose of maintaining the orientation of the specimen is that if a positive margin is identified, it is necessary for the surgeon to know from which area of the surgical cavity to remove more potentially cancerous tissue. The specimen is then x-rayed to confirm tumor inclusion, as demonstrated in Figure I.3.

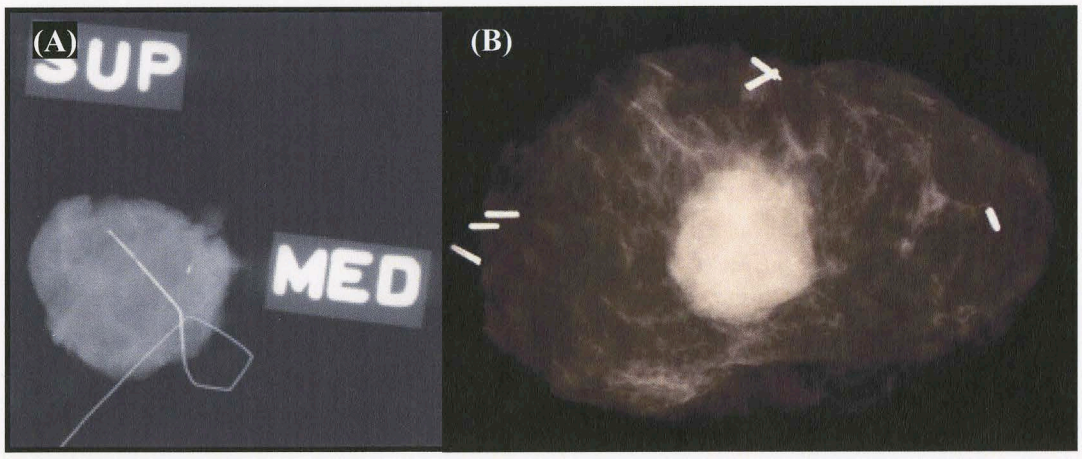

Figure I.3. Radiographs of excised cancerous breast tissue oriented with (A) sutures (Baron, 2000) and (b) clips (Marazzi).

Following this, the specimen is given to the pathologist who fully orients the tumor by replacing the orientation clips or sutures with six colors of differential ink on the areas of specimen corresponding to specific orientation directions: superior, inferior, anterior, posterior, medial, and lateral (Figure I.4). The pathologist then sections, or slices, the specimen by hand in order to examine each slice for a healthy margin of at least 2 mm.

Figure I.4. Differentially inked breast tumor specimen (Pinder, 2005).

The process of intraoperative pathologic examination of a typical surgically excised tissue specimen is illustrated in Figure I.5. The entirety of the intraoperative margin assessment process takes approximately 25 minutes (Uecker, 2011). Because of the high cost of operating room time and the added risk of having a patient under anesthesia for extended periods of time, we aim to significantly reduce this overall processing and assessment time with the introduction of our device.

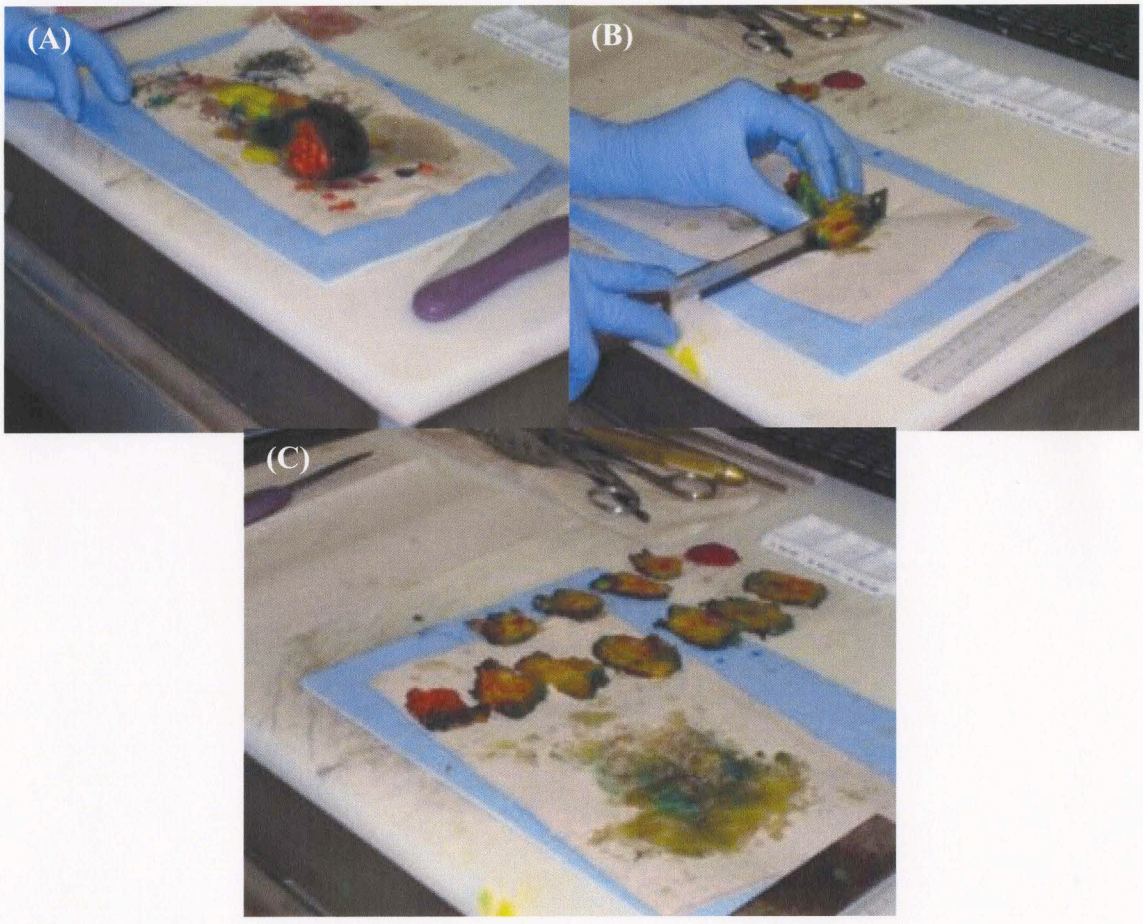

Figure I.5. The current process of specimen assessment; the steps are (A) using ink to orient the whole specimen, B) sectioning of the specimen, and (C) examination of specimen sections.

Limitations of the current gross pathology process

While there have been many improvements in the microscopic examination of tissue (Bankfalvi, 2004) (Cesar, 2007) (Jean-Philippe, 2010), the process of gross examination of specimens has remained relatively unchanged for decades. The current process of tissue examination leads to user-dependent and non-reproducible results, as described by practicing pathologists. Considering the critical importance of intraoperative gross examination in clinical outcomes (Uecker, 2011), the lack of improvements to the process renders it error-prone. We have identified this lack of improvements as a significant current clinical problem. Furthermore, definitive margin status is often not available until well after the patient has left the operating room, another factor leading to the high percentage of repeat surgeries (Uecker, 2011). Delayed assessment is likely due to the fact that (1) some hospitals opt out or do not have the resources for intraoperative assessment of tumors and (2) the gold-standard of margin assessment through microanalysis takes up to several days (Uecker, 2011). Additionally, hospitals that choose to perform intraoperative margin assessment with sub-optimal methods have approximately twice the local breast cancer recurrence rates in patients who select breast-conserving surgery over mastectomy (Atkins, 1972). Specific limitations of current intraoperative pathologic examination devices and techniques include:

1. Inaccurate specimen orientation
2. Single-plane specimen imaging
3. Non-reproducible specimen sectioning
4. Lack of proper specimen fixation

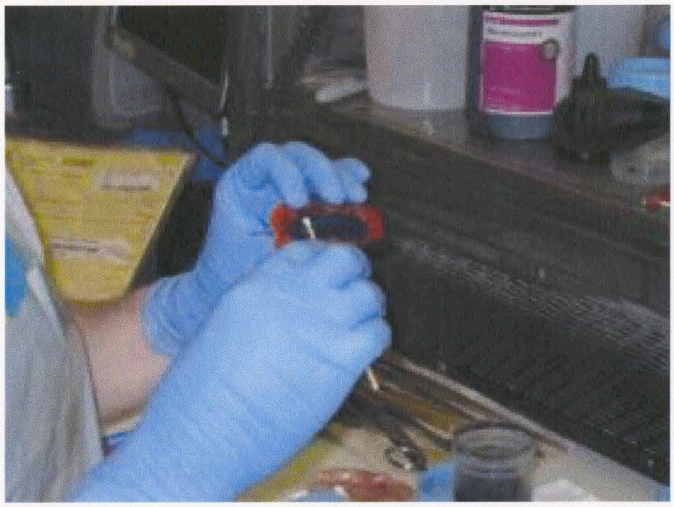

Figure I.6. Process of differential inking of excised tumor specimen.

Handling errors of breast specimens often lead to frequent issues in breast surgery practices (Dooley, 2005). Therefore, it is important to identify and understand all possible sources of error.

Inaccurate specimen orientation

Specimen orientation is the practice of marking the excised tissue specimen as it was oriented in the body prior to surgical removal. The orientation information is of critical clinical importance because the presence of cancer in a particular margin of the specimen guides the surgeon to remove additional tissue from only the corresponding area of the surgical site. This avoids removal of excess healthy tissue, an undesirable outcome for patients choosing a breast-conserving treatment option.

Full specimen orientation is currently accomplished by a process called differential inking, in which each side of the excised specimen is dyed in a different color as demonstrated in Figure I.6. In the case of breast cancer, the American Society of

Breast Diseases recommends that specimen orientation be performed by the surgeon in the operating room during surgery, since the surgeon has the best perspective on orientation (Feldman, 2005). However, in reality, the time-consuming procedure of fully orienting a specimen is not done by the surgeon. Rather, the surgeon places several orientation clips or sutures (Figure I.3) and sends the specimen to the pathologist to complete the process with inking.

Single-plane imaging of specimens

There are no currently-available specimen containers for breast-conserving surgery that offer a mechanism for x-ray imaging specimens in two planes. The power of two-view x-ray imaging is in revealing additional margin information. This issue is exemplified in Figure I.7(A), in which an image is shown with a tumor at the center of the specimen with seemingly adequate margins but, as revealed in Figure I.7(B), the image of the same specimen horizontally reveals a dangerously close margin. At Temple University, where these images were taken, the incorporation of two-view radiography reduced repeat surgery rates from 12% to 5% (McCormick, 2004).

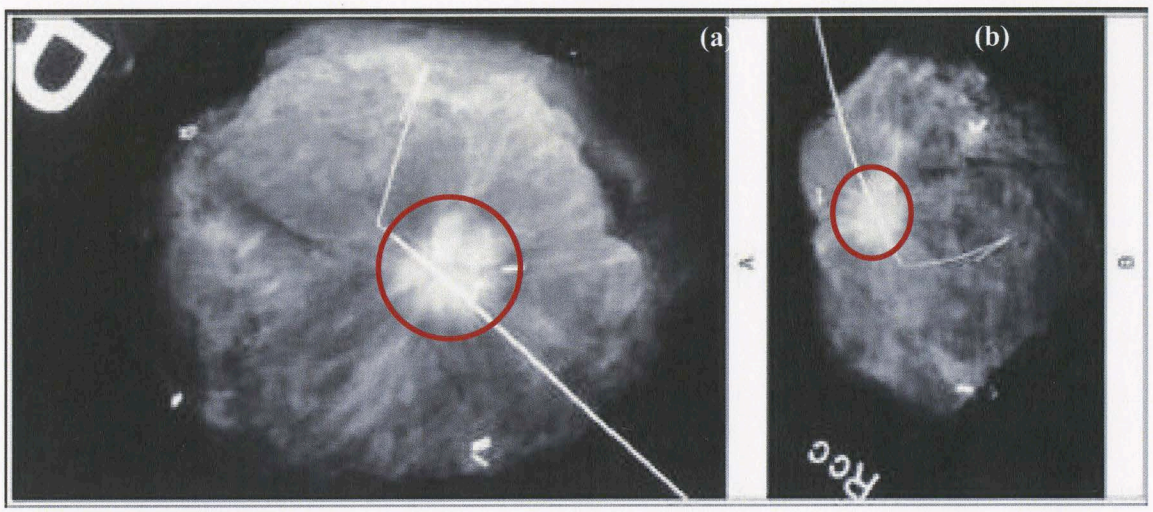

Figure I.7. X-ray images of a breast specimen: (A) vertical and (B) horizontal images of a breast tumor specimen. The bulk of the tumor mass is within the red line (McCormick, 2004).

Non-reproducible specimen sectioning

A major source of error in gross examination of tissue arises from the irregular, non-uniform pattern of cancer growth in tumors, as shown in Figure I.8. Even once the tumor mass is removed, the irregular growths are often present, but cannot be seen with the naked eye or standard imaging modalities (Karssemeijer, 1993).

The implication of this in gross tumor assessment is that, if sections are not cut thinly enough, positive margins may be missed. Standard practice is to section tissue specimens serially every 5 mm (Abe, 2000); but, due to the fatty consistency of breast tissue and the unreliable method of manually slicing, thin and even sections are not always possible. Instead, instability of the tissue during sectioning can result in thick, uneven sections that may not allow for identification of positive margins, as illustrated in Figure I.9. Missed positive margins in gross examination, if caught in further assessment

steps, lead to repeat surgery and, in unfortunate cases where the margin is not caught at all, will likely result in local recurrence.

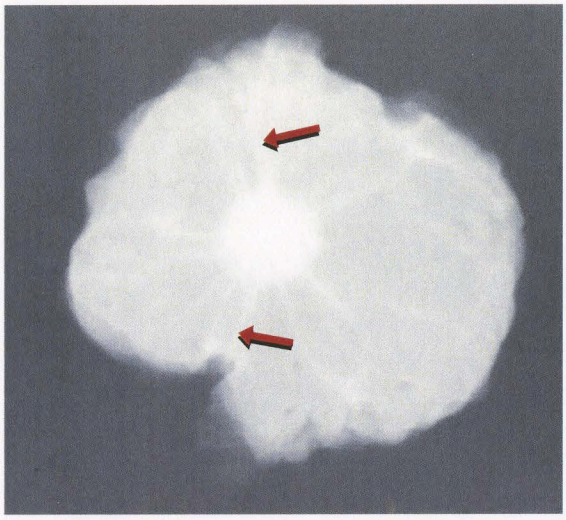

Figure I.8. Radiograph of a breast tumor exhibiting spiculations, at which the red arrows are pointing (Smart-Surgery, 2011).

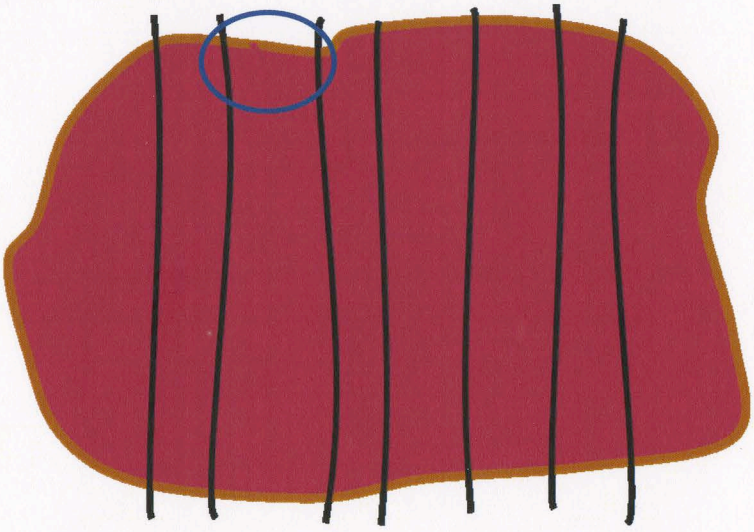

Figure I.9. Illustration of missed positive margin (circled in blue) due to instability of specimen during current method of sectioning. The black lines indicate where sections have been made.

One method to avoid missing cancerous margins is intraoperative cryosectioning, but the limitation of this technique is that the freezing process introduces artifacts that may obscure accurate diagnosis and that may even produce false-positive results (Deyanira, 2009) (Shayan, 2004). Additionally, not all medical centers have the equipment or expertise available to perform frozen sectioning for each case.

A more accurate, but significantly more time-consuming approach to margin assessment is microscopic analysis of fully-processed tissues by the pathologist after surgery. The tissue preparation process consists of the following (Mercer University School of Medicine, 2011):

1. Full fixation of the tissue in 10% formalin for up to 24 hours
2. Placement of the tissue into processing cassettes for dehydration through cycles of alcohol and xylene
3. Paraffin penetration of the tissue
4. Microtoming and placement of the tissue sections onto slides
5. Hematoxylin and eosin staining of the slides

Once these steps are complete, microscopic analysis can be done by the pathologist. The process of specimen sectioning for further microscopic examination is illustrated in Figure I.10 below. Due to the number and length of the steps, definitive margin status often takes days to determine.

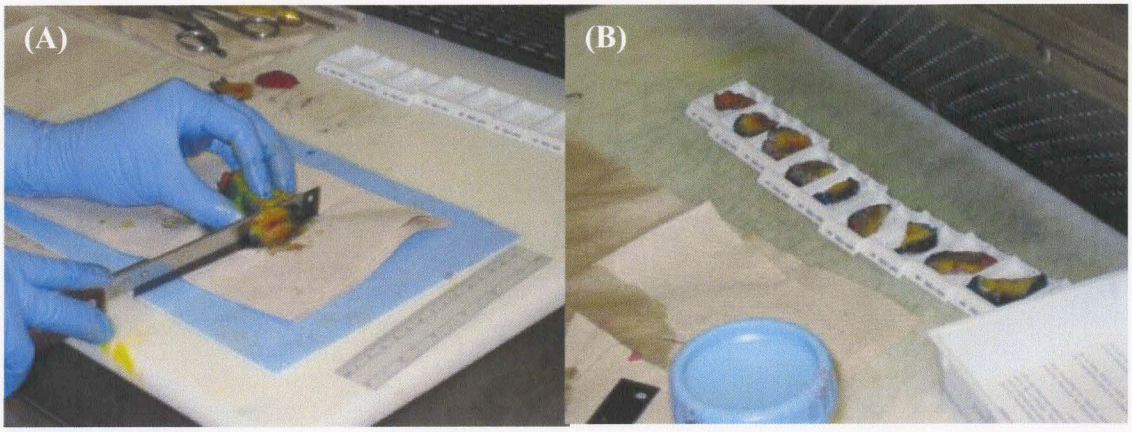

Figure I.10. (A) Manual sectioning of specimen; (B) slices placed in cassettes for further examination.

Lack of proper specimen fixation

Tissue fixation is a critical part of tissue processing. Following gross examination of the excised tissue, specimen slices are typically wrapped in a paper towel and placed in a solution of formalin, as shown in Figure I.11. Generally, tissue fixes in 10% neutral-buffered formalin at an approximate rate of 1 to 2 mm per hour (Tangella, 2010). Because the process of cellular breakdown and decay begins the moment that the tissue is removed from the body (University of Washington School of Medicine, 2012), fixative penetration is pertinent. 10% formalin is used largely because of its ability to rapidly penetrate tissue, however, for thick specimens, autolysis and putrefaction is still likely to occur leading to artifacts in the tissue (Specht, 2001). The device described in this document has been designed in order to minimize tissue thickness, thereby decreasing the risk of cellular breakdown before the fixative has penetrated.

Figure I.11. Tissue section is wrapped in a paper towel and placed in a container of formalin.

Current Tools for Intraoperative Margin Assessment

There are a number of tools being developed to improve the process of intraoperative positive margin detection. These tools are largely hand-held fiber-optic probes that use varying optical techniques to identify cancerous cells within a ~2 mm margin of excised tissue. Mahadevan-Jansen et al. (2011) is developing spatially offset Raman spectroscopy (SORS), a method to detect subtle changes in soft tissue spectra in the 100-2000 pm range, to be tested on excised breast tissues. In another study, MALDI mass spectrometry, a molecular technology that has the specificity and sensitivity to monitor and identify cellular changes in renal carcinoma, was successfully used to assess differences between a tumor and adjacent normal tissue (Oppenheimer, 2010). Similarly, Keller (2010) and Kennedy (2010) took spectral measurements from the surface of the

breast tissue masses following excision in order to examine the use of autofluorescence, diffuse reflectance spectroscopy, and spectral imaging in evaluating margin status intraoperatively; Keller et al. were able to identify positive margins with 85% sensitivity and 96% specificity. These tools are being designed to optimize *detection* of cancerous margins. In contrast, our device is designed to improve upon the current gross examination process itself with the goals of reducing both the excessive removal of healthy tissue and the incidences of repeat surgery and local recurrence of cancer. There are a number of promising advances being made in this area of intraoperative margin assessment, but adoption of these aforementioned tools by the medical community has been limited.

Speaking with physicians from various hospitals around Tucson, we discovered that there are two major reasons for limited adoption of many medical tools: cost and resistance to change. Hospitals, like all public and private operations, have limited budgets; therefore, purchases for new equipment are not made unless deemed necessary. Necessity, in this case, refers to the long-term difference the equipment will make on the cost of treating a patient. For example, if Equipment X statistically decreases the need for repeat surgeries, then the hospital will end up saving money on operating room time, and the investment is worthwhile for the facility. Additionally, physicians, like most people, are resistant to adopt novel technologies once standard practices have been established due to the learning curve associated with new techniques.

The most comparable tool that is currently being used for intraoperative margin assessment is similar to the gel component of the technology that will be described in this

report. The Tissue-Tek Optimal Cutting Time (OCT) compound is a water-soluble gel composed primarily of polyvinyl alcohol and polyethylene glycol; it is currently being used by research facilities worldwide for the purpose of embedding tissues for improved speed of frozen sectioning and analysis (Gene Research Lab). The method by which it is used is as follows: a tissue section is placed into a specimen block and is then fully covered with the OCT compound; the compound infiltrates the tissue and binds it to the block at which point the tissue block is placed in liquid nitrogen. The tissue can then be thinly and evenly cryo-sectioned and examined for positive margins. Although the use of this compound is similar to the one proposed in this document, there are limitations to the OCT compound that are addressed by the technology described in this document.

As mentioned earlier, frozen sectioning, even when done in a controlled manner whereby thin and even sections are obtained, is limited by the potential tissue artifacts produced during freezing. These artifacts have been found to obscure diagnosis in some instances (Deyanira, 2009) (Shayan, 2004). Furthermore, the additional capital equipment that is necessary to produce frozen sections is a limiting cost factor in the adoption of this technique in hospital settings.

Keeping in mind the limitations of current practices and tools, we aimed to design a device for the purpose of providing a simple, affordable method of intraoperative margin assessment that does not requirement significant changes in current practices by both the operating surgeon and the pathologist.

In the following studies, the characteristics and considerations that went into the mechanical design of the device hardware will be described in a manner that addresses

the limitations of current tumor specimen orientation practices. Following this, the novel gel properties and components will be described in detail with emphasis on current related applications. Then, three studies involving the testing of specific device properties will be reviewed. The first study examines the time needed for various gel formulations to set and the maximum temperature reached during this reaction in order to evaluate which formulations would be most suitable for intraoperative applications. The second study looks into the radiographic properties of the gels and potential plastic materials for the hardware for the purpose of eliminating materials that may interfere with x-ray lesion assessment. The purpose of the final study is to assess if the gels have any effect on the processing and analysis of cancerous tissue. The results of these studies will determine the potential for this device to be used in a clinical setting and will lay the foundation for future applications.

II. PROPOSED DEVICE AND PROCEDURE FOR TUMOR SPECIMEN PREPARATION

The aforementioned limitations of current intraoperative gross examination methods were first pointed out to us by breast pathologist Dr. Lauren Grasso at the University Medical Center. She identified the user-dependence of the process, the excessive amount of time that full gross assessment adds to an operation, and the lack of significant improvements over decades in the area of gross examination. Dr. Grasso also emphasized the substantial resistance to change that is present in her field. Using this knowledge of the specific limitations of current practices and the necessity to develop a tool that supplements current techniques rather than replaces them, our team, consisting of Emre Toker, an electrical engineer, Mark Banister, a polymer chemist, Dr. Grasso, and myself, began to design and develop the unique aspects of the device.

The device consists of two main parts: the hardware and the gel. The gel component was contributed by Mark Banister who was in the midst of developing the polymer mixture for his company, Medipacs. Its original application was in a swelling, hydrogel-based drug delivery system but its properties of biocompatibility and rapid setting made it optimal for our application; and, as described in future sections, we have been able to optimize it for our purposes. The device hardware, on the other hand, has gone through several revisions since its original inception. Initially, the design was significantly more complicated than the design presented in this report. It contained the following features which I have since deemed unnecessary:

- A flexible base for the purpose of looking at the tissue specimen sections without removing them from their original conformation
- A sectioned base in which each section (of approximately 15 in total) could be independently removed then replaced following tissue assessment
- Plastic sectioning guides that attached on each side of the base sections allowing for even tissue section thicknesses during slicing

After conducting more research into the current practices of margin assessment, both gross and microscopic, I identified that these features are not only unnecessary but would potentially interfere with current tissue processing and assessment methods. The specimen sections must be removed from the original conformation in order to analyze each section thoroughly for positive margins; additionally, there is no need to replace the sections following assessment because the entire tissue section is immediately processed for microanalysis. Lastly, any plastic that is in the gel, such as the proposed sectioning guides, would have to be removed before processing because plastic cannot be microtomed, a necessary step in preparing tissue for microanalysis. Since our initial work, I have simplified the structure of the hardware and added functional features that address all limitations of assessment practices described previously without interfering with processing of the tissue.

A. Device Hardware

As described in Section I.B., limitations in orientation practices can result in the excessive removal of healthy breast tissue, inaccurate margin assessments, and

unnecessary repeat surgeries. The device hardware is designed to address the limitations associated with orientation of excised tumor specimens.

The specific purposes of the device hardware are (1) provide useful orientation information for the surgeon in the operating room, (2) provide orientation information in the radiograph for the physician assessing x-ray tumor inclusion, and (3) provide features for the pathologist to maintain orientation through the gross examination process. In creating the features of the mechanical design, we went through a number of steps.

The process began by identifying the optimal shape of the device. Due to storage limitations in hospitals, a cubic shape was decided upon. Orientation markings were added in a manner that would reflect breast positioning in the operating room; since the patient lies horizontally on her back, we designed the top plane, or opening of the cube, to correlate with the direction of the nipple. The directionality medical terms ("Superior", "Inferior", "Medial", and "Lateral") were embossed on each side wall of the device. In order to minimize the amount of change for the surgeon, it was necessary to emulate the current orientation practice (Figure I.3). We added three different length pegs that can be seen clearly from above to correlate with the current technique of using three sutures of different lengths; the short peg corresponds to the "SUPERIOR" orientation direction and the middle and long length pegs correspond to the "MEDIAL" and "LATERAL" orientation directions, respectively. The orientation markings and pegs can be seen in Figure II.1(A).

Another concern that pathologists discussed during our interviews was that of orientation once the gel is sectioned. In order to section the gel, the hardware walls will

be folded down and the orientation markings used by the surgeon would no longer be present. The concept of embedding shapes (e.g. circles, triangles, squares) corresponding to orientation directions addressed this concern. Once the gel hardens, the hardware will have embedded the edges of the gel with pertinent orientation information to the pathologist, as illustrated in Figure II.1(C).

It is necessary to have orientation information available in the radiograph as well for the purpose of initial margin assessment. In order to address this need, we have integrated markings designed to be visible on an x-ray; an "S" and "L", corresponding to 'Superior' and 'Lateral', respectively, are present, as shown in Figure II.1(B). In addition, we have added a row and column for the purpose of identifying the specific area of the tissue in which the mass is present (Figure II.1(B)). Radiographic orientation information is also available on the "SUPERIOR" wall, allowing for imaging and orientation in an additional x-ray plane.

As aforementioned, it is necessary for the walls to open and collapse down in order to facilitate sectioning, or slicing, of the gel-encapsulated tissue by the pathologist. The major difficulty associated with the design of this feature is that the cube cannot be designed intact. Due to factors such as cost and mold longevity, we have chosen to create a straight-pull mold—a mold that requires mechanical designs in which two halves of the mold pull straight away from each other. An example of a straight-pull mold is shown in Figure II.2.

In order to create a design that allows for this type of molding to be done, an unfolded cube was created. To allow for re-folding of the cube, very thin (1 mm) plastic

was made to connect the walls to the base of the cube (Figure II.1(D)). Once the flat cube is injection molded, the walls will be folded up and glued together, giving the device its cubic shape.

A requirement for optimal gross assessment is the sectioning of thin (5 mm) tissue slices (Weidner, 2003). From the observation of current practices, it has been noted that pathologists use no quantitative method of measuring the sections. We designed sectioning marks that are spaced every 5 mm; once the gel hardens, the marks will be embedded into the gel, serving as guides for the pathologist to follow (Figure II.1(D)).

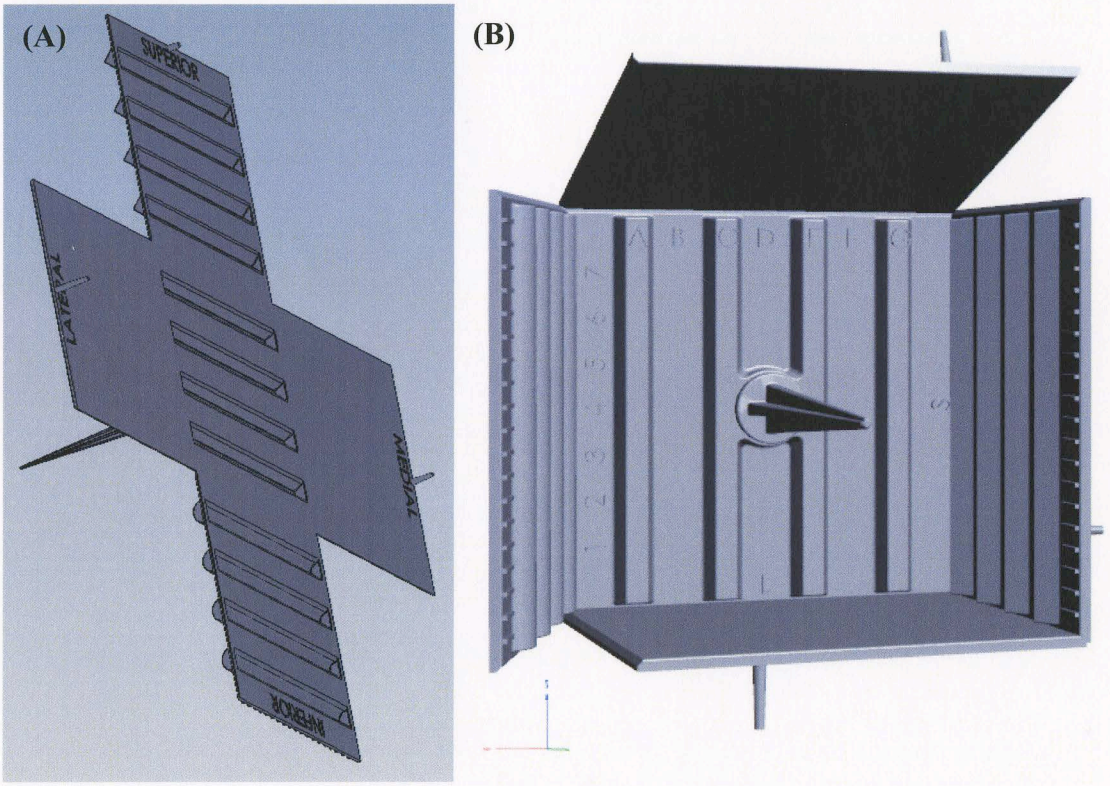

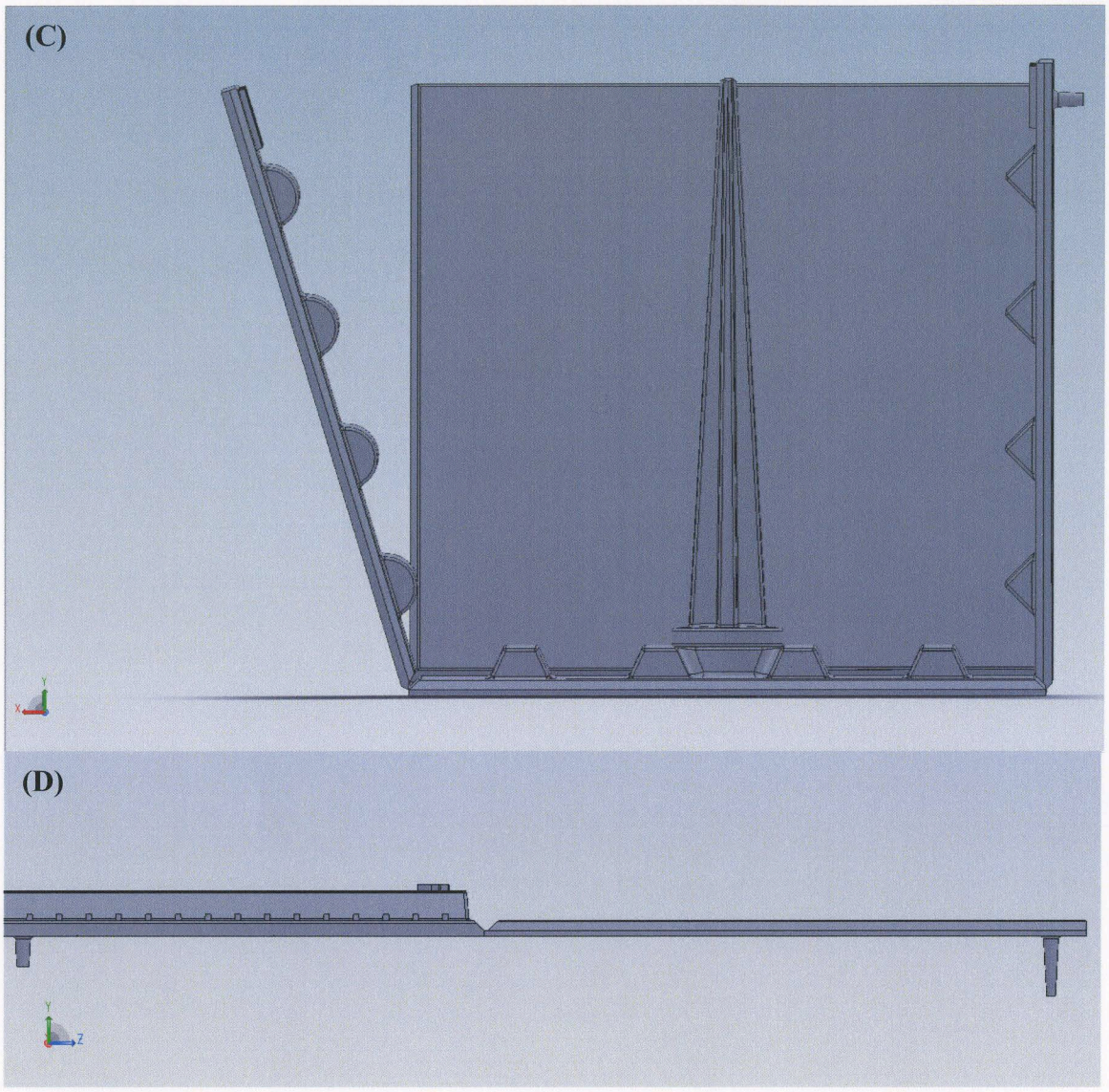

Figure II.1. Different angles of the device hardware mechanical design. The following features are visible: (A) the medical orientation markings, (B) x-ray orientation markings and top-view pegs, (C) the embedded shapes for orientation of the specimen once the hardware is removed, and (D) the 1 mm thin plastic connecting the wall to the base and the 5 mm spaced sectioning guides.

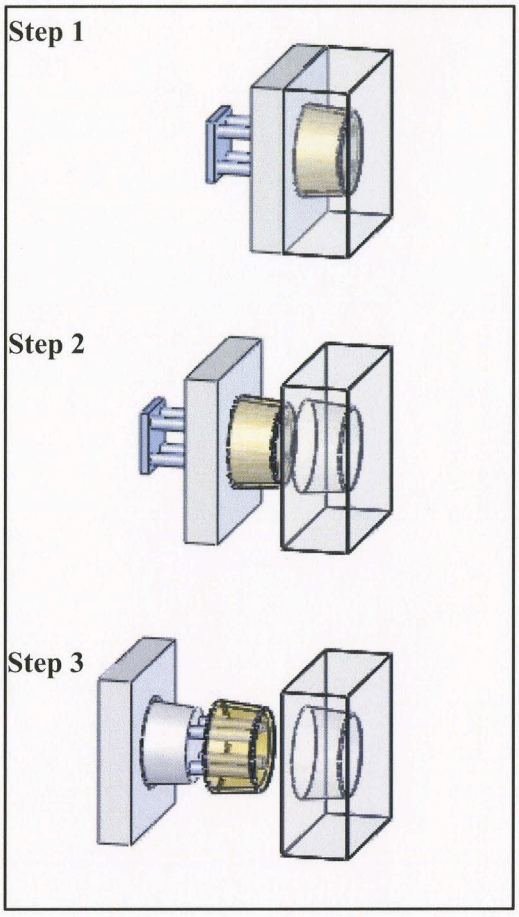

Figure II.2. The steps taken to create a straight-pull mold (ProtoMold, 2011).

In addition to the design parameters necessary for device functionality, it was also necessary to take into account the feasibility of mold creation. The device was modeled with draft angles of at least 0.5˚, a requirement for simple, straight-pull molds. Also, for this type of mold, depth of features is limited. Our only deep feature is a centered tissue anchor. In our preliminary tests in which we placed tissue into an unhardened gel, the tissue, due to a difference in density, floated to the surface of the gel. If this happens in a clinical setting, key orientation may be lost. The anchor, see in Figure II.3 with a 5 mm diameter base, is designed to pierce into the excised tissue mass, thereby holding it in

place until setting occurs. In reality, the anchor will have to be significantly thinner in order to pierce the tissue without causing morphological damage to the specimen. The anchor will be approximately the thickness of a 12-gauge needle. It has been designed to be injection molded separately and then tightly fastened into the cube once molded. In order to accomplish this, the base of the device was designed with an elliptical hole matching the base of the anchor, shown in Figure II.3(A). Once the tissue anchor is placed in the hole, a clockwise turn fastens it in place and two protruding wedges, shown in Figure II.3(B), hold the structure in place. It will be necessary to select a material that is strong enough to withstand the tissue piercing process without fracture to the anchor. We will test this property experimentally once a prototype is ready to be built.

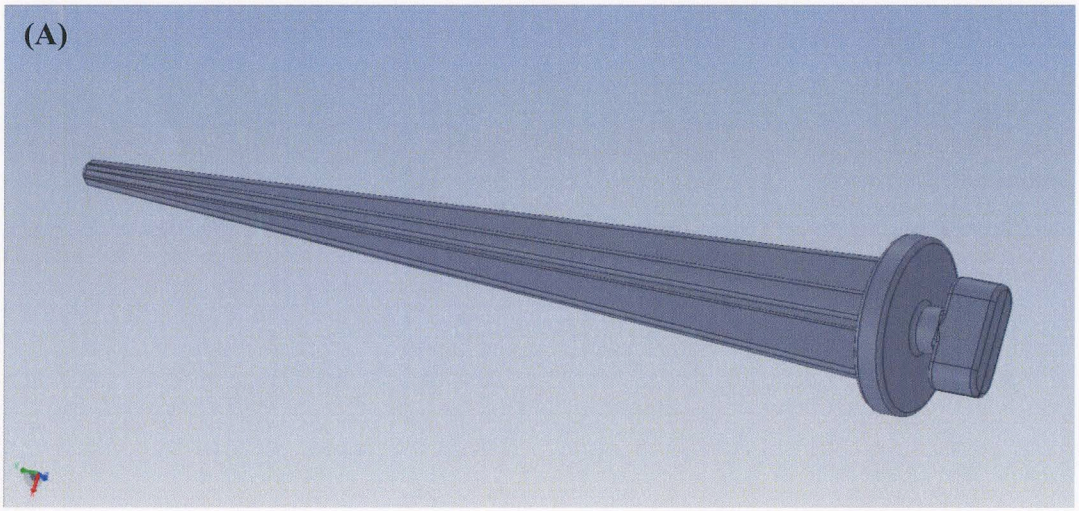

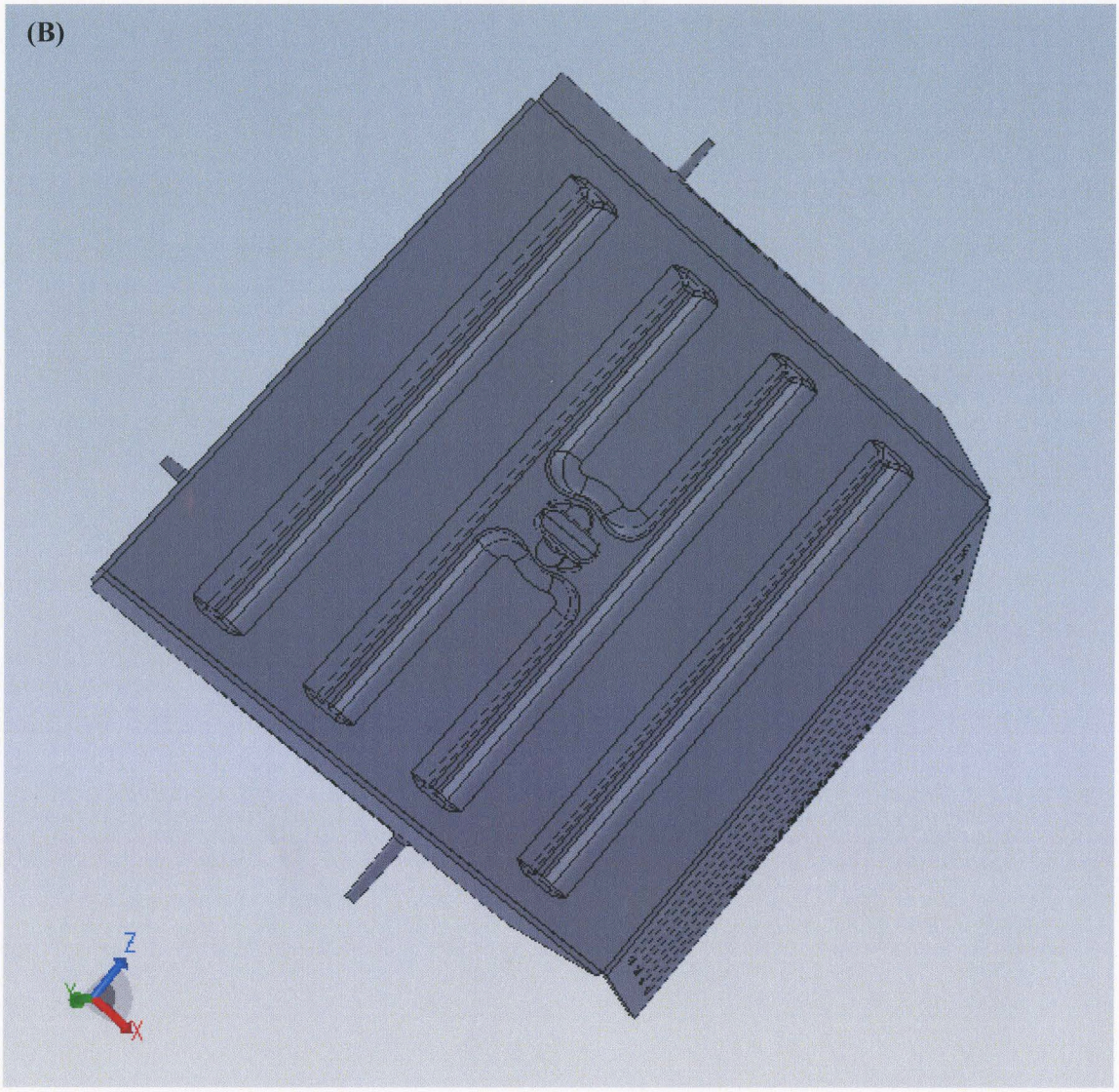

Figure II.3. Mechanical design of (A) the independently-molded tissue anchor with appropriate draft angles and (B) the device base where anchor is inserted and fastened into place.

Several features of the hardware are designed to provide support and shape for the gel in the steps following initial orientation and radiographic assessment. The next section will go into specifics regarding what materials constitute the gel and their uses in intraoperative breast cancer examination.

B. Device Gel

Novel properties and current uses

The novel gel formulation created consists of the following two polymers: poly(ethylene glycol) diglycidyl ether and poly(ethyleneimine), with water used as a solvent; both polymers are obtained from Polysciences, Inc. Before settling on this compound, we tried several other materials including a variety of cyanoacrylates and UV-curing resins. The cyanoacrylates set in a manner of minutes but are limited by the fact that, when used in volumes greater than 5 ml, the temperature of the reaction was so high that the materials could not be handled. Additionally, the hardened materials were too rigid to be cut easily by hand. The UV-cure resins are desirable because of their ability to cure in less than 1 minute. The major limitations of these materials are (1) in order to be utilized for intraoperative applications, additional equipment, a high-powered UV lamp, must be introduced to an already space-limited operating room and (2) additional work must be done by the operating room staff to ensure full setting of the material. In comparison, the combination of poly(ethylene glycol) diglycidyl ether and poly(ethyleneimine) in water results in an independently and rapidly setting hydrogel that is biocompatible and can be easily sliced by hand.

Poly(ethylene glycol) diglycidyl ether (PEGDE) is a derivative of the poly(ethylene glycol) group. This group of polymers has found numerous uses and applications due to its water solubility, hydrophilicity, physiological inactivity, low toxicity, and stability under varying chemical conditions (Polysciences, Inc., 2007). Applications of poly(ethylene glycol) polymers range include industrial practices such as

ink solvents and dispersants (Zopes, 2010), separator and electrolyte solvent in lithium polymer cells (Lee, 2001), polar stationary phase for gas chromatography (Gu, 2011), and surfactants (Kausik, 2011) (Kumar, 2011) as well as medicinal applications such as precipitants for plasmid DNA isolation (Baeyens, 1994), virus concentrators (Hitchman, 2011), and stabilization agents for gene therapy vectors such as viral plasmids and liposomes (Kreppel, 2007) (Rossi, 2006) (Geisbert, 2010).

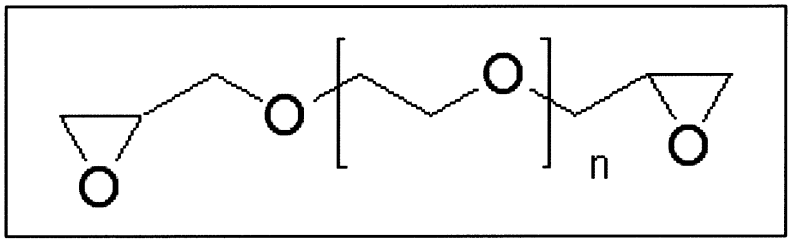

Figure II.4. Chemical structure of poly(ethylene glycol) diglycidyl ether.

Poly(ethyleneimine) (PEI) is an organic polymer that contains a high density of primary amines. Its polycationic nature lends itself to various biological applications such as cell attachment promoters (Vancha, 2004), transfection reagents (Rudolph, 2000), and as cytotoxicity agents (Moghimi, 2005). When combined with water, the PEGDE and PEI crosslink to form a biocompatible, ductile gel that is very suitable for our applications. The reaction, shown in Figure II.6, is the result of the amine groups on the PEI bonding with the epoxy groups on the PEDGE creating a highly cross-linked hydrogel. The exothermicity of the reaction is due to the breaking of the epoxide rings during bonding (Antoniotti, 2004).

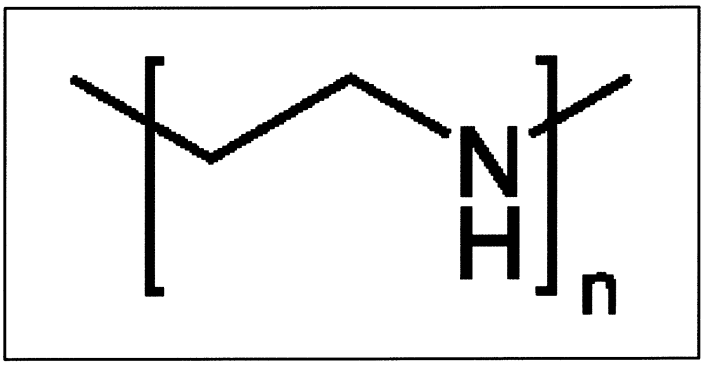

Figure II.5. Chemical aminated structure of poly(ethyleneimine).

Current applications that use a combination of PEI and the derivative ethylene glycol diglycidyl ether are primarily in coatings and applications such as surface-ion imprinting (Li, 2011), nanoparticle cross-linking (Goyal, 2011), formation of sterically stabilized polystyrene latexes (Walsh, 2010), and complex cell-micropatterning (Yamazoe, 2009). Additionally, there has been significant work done in the area of hydrogel actuator development. Banister et al. (2007) has designed and tested formulations of electroactuated polymer hydrogels for the purpose of controlled drug delivery via pump. They found that varying the fraction of reactive components affects the hydrolytic instability of the hydrogels, brittleness, and equilibrium swelling ratio. In this study, we use a similar method of component variation in order to use the reaction to optimize properties for our uses.

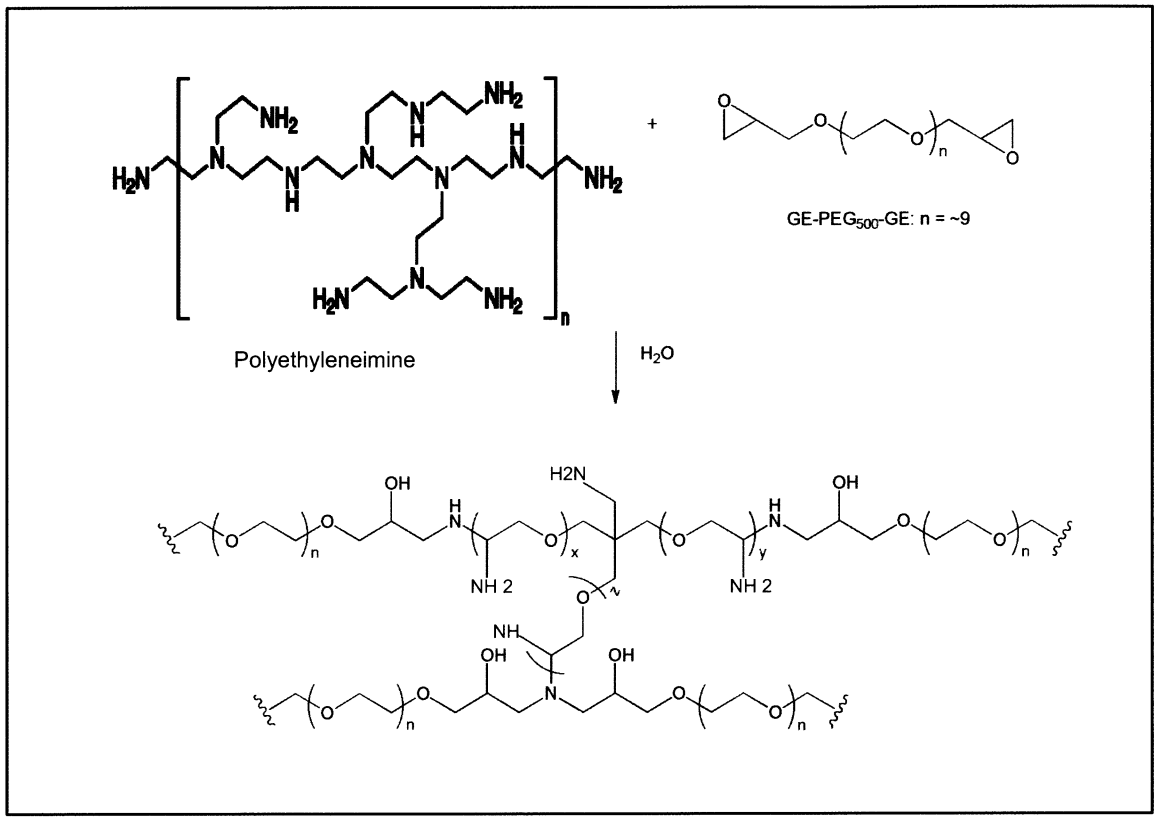

Figure II.6. The chemical reaction between the three components of the gel mixture, PEI, PEGDE, and H_2O.

It is important to note that gel swelling does occur in the formation of hydrogels. The extent of swelling is dependent on the density of the polymeric mesh where water molecules fill the gaps in between the polymer chains. Swelling is therefore dependent on variables such as the chain lengths of the polymers and the ratio of the components in each formulation. For our purposes, swelling is of little concern due to the structure of our hardware; since the top of the device is open, any swelling-induced volume change will result in gel translation upwards, with likely no effect on the encapsulated tissue specimen.

Device gel uses

The purpose of the gel formulation in this application is to (1) eliminate the need for differential inking of specimens by holding orientation information in its shape and (2) provide support for the specimen during sectioning.

As shown in Figure II.1, the hardware details the specific orientation information for the surgeon and pathologist. However, the hardware itself does not keep the specimen in its proper orientation. The gel has been designed to be poured into the hardware; then, minutes after the specimen has been placed inside by the surgeon in the operating room, it sets into a hardened but moderately ductile gel. The entire device with specimen and gel can then be radiographed.

Following radiography, the device is transported to the pathologist. The walls of the hardware are folded down and the 5 mm-spaced sectioning guides that are embedded in the gel allow the pathologist to cut thin, even slices through the tissue and gel material. The sectioning guides coupled with the stability that the gel provides the tissue during slicing minimizes risk of missed positive margins, as is illustrated in Figure II.7. Once the specimen margins are evaluated and any additional cancerous tissue is removed from the patient, the entire tumor and surrounding gel can be fixed, processed, and microscopically analyzed.

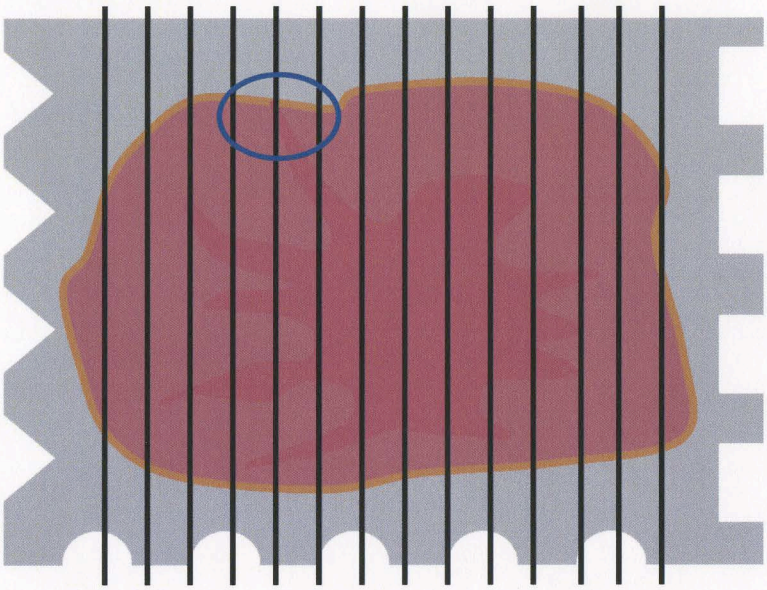

Figure II.7. Gel used to stabilize the tissue to allow for thin, even slicing of the tumor. A positive margin is identified within the blue circle.

The gel property of greatest importance is the time in which it takes the gel to set, or harden. The cost of operating time can be upwards of $130 per minute, not including extra resources specific to the procedure (e.g. clip for an intracranial aneurysm) or surgeon and anesthesia provider fees (Macario, 2010). We are aiming to not only increase the accuracy of the examination procedure but also to minimize the amount of time, and therefore cost, necessary to determine intraoperative margin status.

III. PRELIMINARY TEST RESULTS FOR PROPOSED DEVICE MATERIALS

We designed a study for the purpose of narrowing down the options for gel formulations that would be suitable for intraoperative applications. As aforementioned, the function of the gel itself is to (1) to keep the specimen in its proper orientation and (2) to provide stability to the tissue during sectioning.

The gel property of greatest interest is the setting time. A major factor that is always taken into account in surgical procedures is operating room time, due to both patient safety and cost. Because many surgeons opt to get margin assessments of lumpectomies intraoperatively, the amount of time that it takes the gel to set is of utmost importance.

Based on our observations of the pathologists' inking and sectioning process in the operating room, the current process takes between 10-25 minutes depending on the tissue size and consistency, the physician's experience, how the surgeon has oriented the specimen, as well as other potential factors. Our device not only aims to remove sources of human error, such as multiple persons orienting a specimen, but also to shorten the amount of time necessary in the operating room. We aimed to identify the gels with properties that would enable this.

We began by outlining 32 target gel formulations, varying both the volumes of the components as well as the chain lengths of the two polymer components, as outlined in Table III.1.

Table III.1. Gel formulations with the chain lengths and volumes tested.

Gel #	**PEI chain length**	**PEGDE chain length**	**PEI** (g)	**PEGDE** (g)	**H2O** (g)
1	1200	526	7	5	6.5
2	1200	600	7	5.9	7
3	1200	1000	7	9.5	6.5
4	1200	600	8.4	5.7	7
5	1200	1000	8.4	9.5	6.5
6	1800	526	9.33	5	6.5
7	1800	600	9.33	5.7	6.5
8	1800	1000	9.33	9.5	6.5
9	1800	526	11.6	5	6.5
10	1800	600	11.6	5.7	6.5
11	1800	1000	11.6	9.5	6.5
12	1200	1000	8.4	7.6	6.5
13	1800	1000	11.6	7.6	6.5
14	1200	1000	8.4	6	6.5
15	1800	1000	11.6	6	6.5
16	800	526	3.5	5	8.5
17	800	600	3.5	5.7	8.7
18	800	600	4.2	5.7	8.5

19	800	600	3.5	5.7	10.1
20	800	526	4.2	5	8.5
21	800	600	4.2	5.7	8.5
22	800	600	4.2	5	8.5
23	800	600	5.1	5	10.1
24	800	600	4.2	5	8.5
25	1800	600	11.6	4.7	7.6
26	1200	600	9.3	4.7	7.6
27	1200	526	8.7	7.5	3.5
28	1200	600	8.7	5	5
29	1200	600	8.7	8	3.5
30	800	600	4	5.7	8.5
31	800	600	4.5	4.5	8.5
32	800	600	5	5	8.5

A plastic bag was placed into a 100 mL beaker in order to prevent the gel from sticking to the glass walls. Respective volumes of the components were then added to the beaker, PEI being added first followed by PEGDE, and then lastly water. The contents of the bag were all stirred for approximately 30 seconds and a timer was started. A thermometer was placed into the center of the mixture and the beginning and peak temperatures were recorded. Once the gel fully set, as confirmed by manual prodding of

the surface, the gel was removed from the beaker and bag then cut in half to confirm the center of the formulation was set as well. This was repeated four times for each gel formulation.

The results of the setting times and peak temperatures reached during setting are demonstrated in Figure III.1 below.

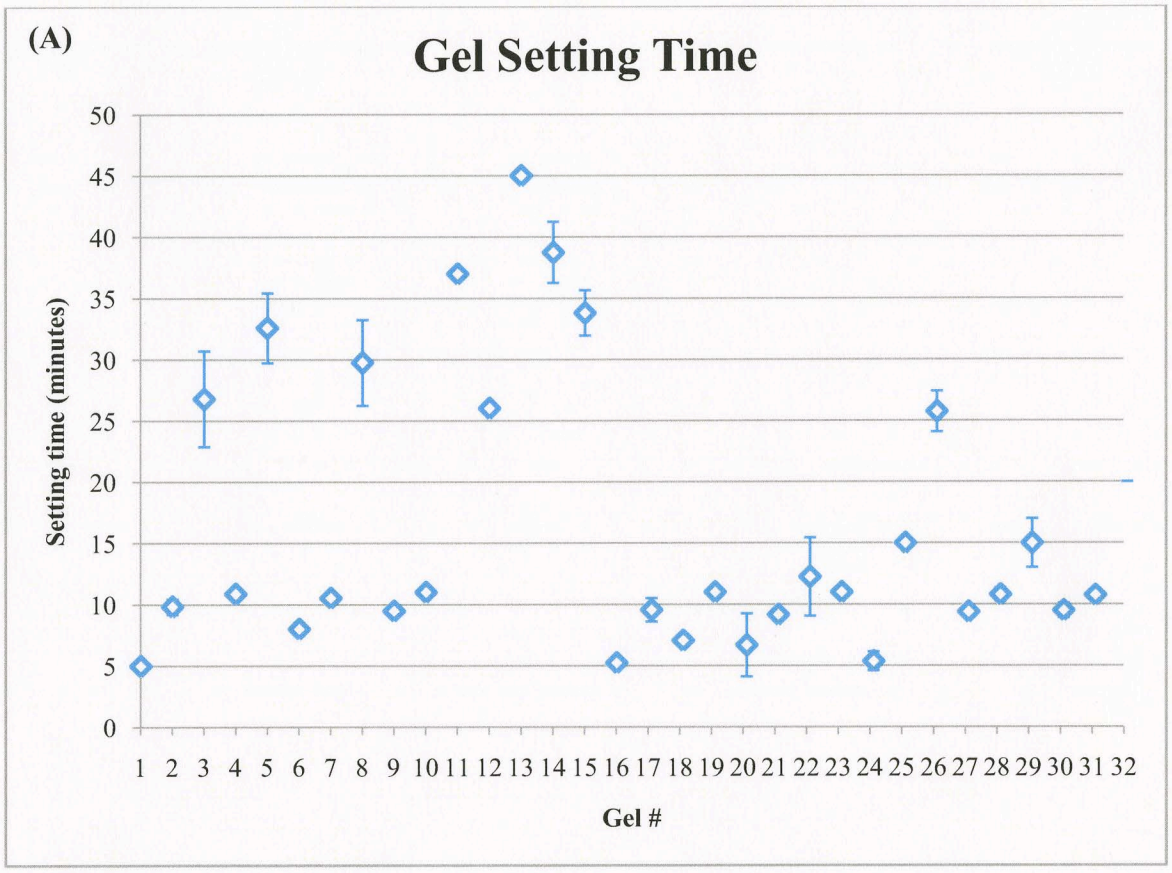

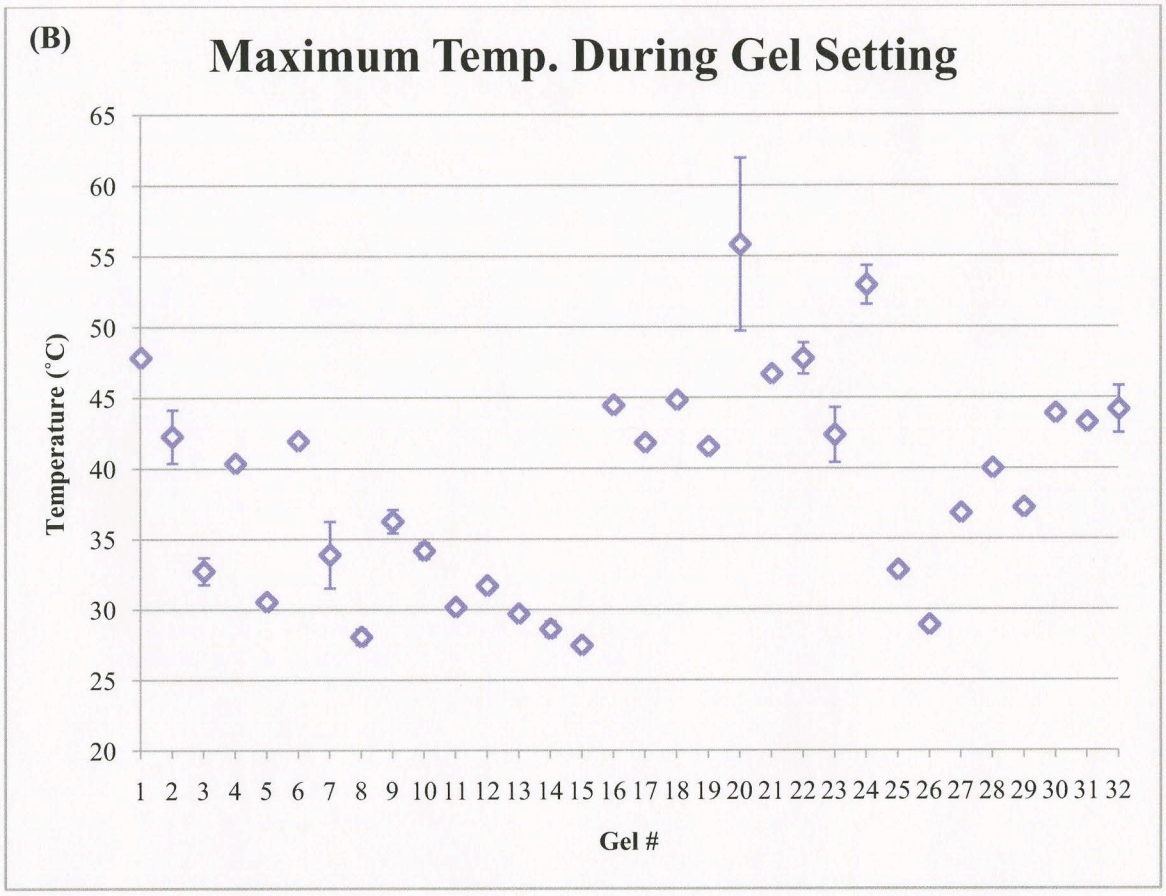

Figure III.1. (A) The total time taken for each gel formulation to set; (B) The maximum temperature reached during setting for each respective gel formulation. The points represent the average value of 4 trials for each formulation with the error bars representing the standard deviation.

Figure III.1(A) demonstrates the wide range of setting times from approximately 5-45 minutes. As previously described, the aim is to identify the gels that have the potential to shorten the current process of intraoperative assessment; therefore, the gels of most interest are those setting under 10 minutes. We identified 11 gels in this range.

Temperature is a significant factor to note due to the effect of thermal exposure on tissue. Notable thermal damage to human tissue varies with both the peak temperature and duration of the thermal exposure (Dewhirst, 2003). We estimate that the duration of

the peak temperature while setting is no longer than 1 minute therefore the maximum temperature that the gel may reach during setting is 54°C (Moritz, 1947) (Stoll, 1959). Only gel formulation #20 reported peak temperatures above the threshold for tissue damage.

We also used the data to compare how setting time correlates to the peak temperature reached when the mixture is reacting. We found that there is a negative correlation; as the setting time increases, the peak temperature reached decreases, as illustrated in Figure III.2.

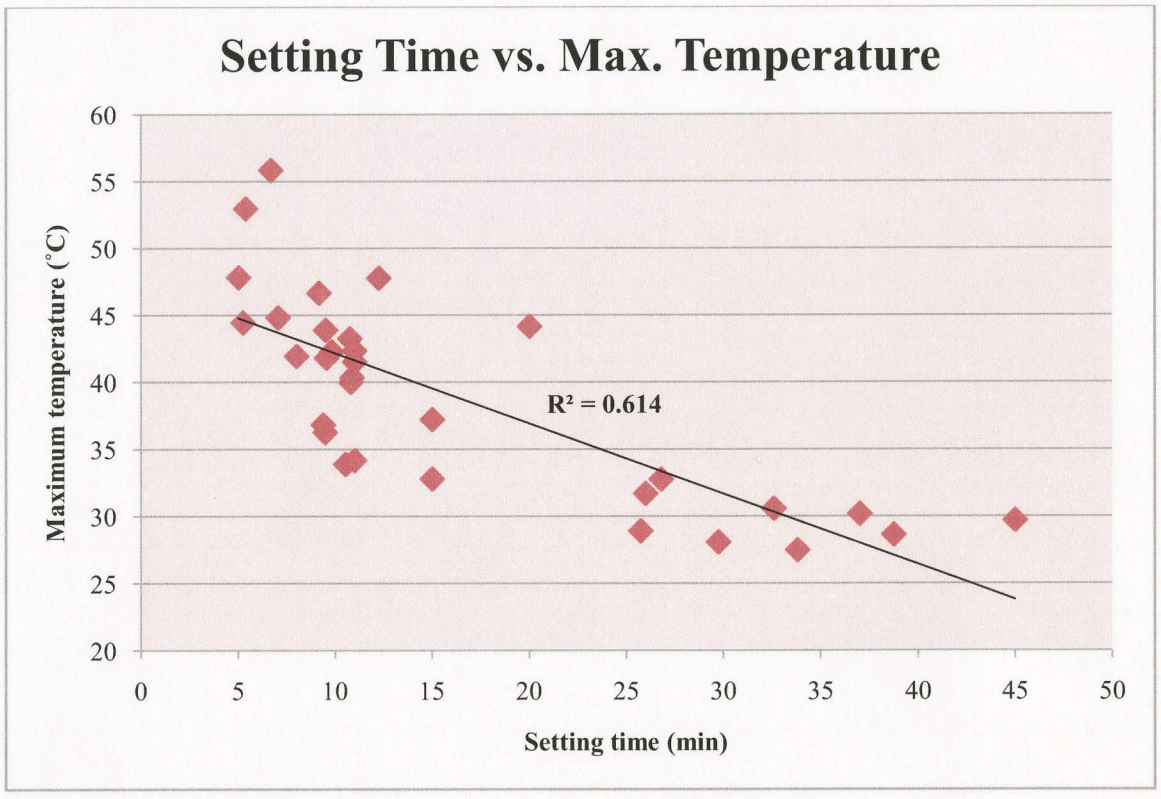

Figure III.2. Correlation between gel setting times and respective peak temperatures reached during setting.

We hypothesized that the setting time is affected by the total volume of the gel mixture due to the decreased ratio of surface area to unit of gel as the total volume increases; as the ratio decreases, heat exchange also decreases. Therefore, it is likely that the temperature of the reaction, and subsequently the setting time, will change with volume. We tested this by preparing a fast-setting gel, #16, at four different volumes and monitoring the temperature profiles at various time points. The formulations were mixed together by the same method as the previous setting time experiments with ratiometric increases in volume. The results are presented in Figure III.3. We found that as the total volume of gel decreases, the maximum temperature reached decreases and the setting time increases.

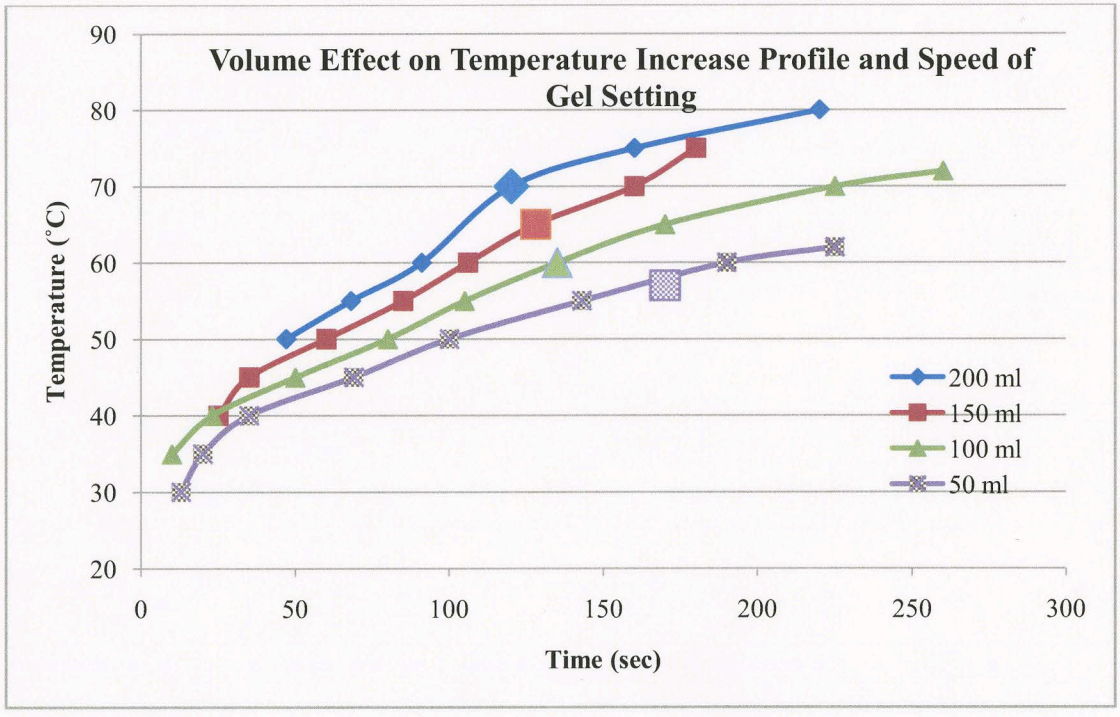

Figure III.3. The effect of volume on the temperature profile and setting time of gel formulation #16. The large point in each set indicates the time of gel setting.

Because there is variation in the size of excised lumpectomies (Kearney, 1995), there may be need to use different formulations for different sizes in order to ensure optimal set times with no thermal damage. The gel tested in Figure III.2 is not suitable for larger specimen volumes due to the potential thermal damage that could be caused during gel setting. We chose to examine other options for larger specimens. We tested two additional 200 ml formulations, #13 and #32, both of which had initial set times of over 15 minutes. In an effort to decrease the maximum temperature of the reaction, we also tested gel #16 again but changed the order in which we mixed the components together. We observed that mixing H_2O and PEI together caused an exothermic reaction, emitting heat; this is likely due to protonation of the PEI amine groups (American Chemical Society, 2011). We therefore mixed these components together first, waited one minute, and then stirred in the PEGDE. The formulations' temperature profiles are plotted against time in Figure III.4.

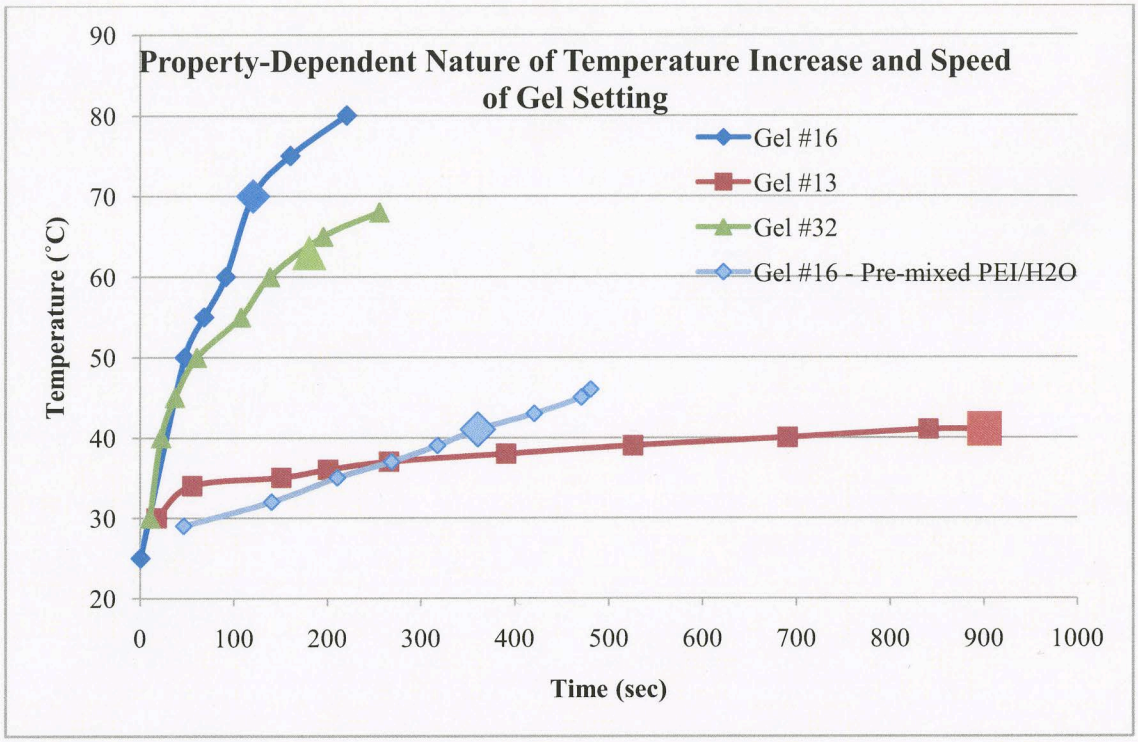

Figure III.4. The effect of volume on the temperature profile and setting time of gel formulation #16. The large point in each set indicates the time of gel setting.

Although setting very rapidly, gels #16 and #32 reached temperatures that are potentially damaging to tissues and therefore could not be used for specimens of this volume. Gel #13 peaked at relatively low temperature of 42°C but it undesirable due to the length of reaction time. As predicted, Gel #16 with pre-mixing of H_2O and PEI, resulted in a slowed setting time of approximately 6 minutes, with a temperature that is suitable for tissue viability. These findings indicate that different gel formulations may be suitable for different volume applications and also that specific gel reactions can be slowed by changing the order in which the components are mixed.

In reality, the temperature reached during the reaction is not likely to present limitations for our device in this proposed application. High thermal exposure to the

surface of the excised tissue sample may cause apoptosis or necrosis to the first few layers of cells but tissue morphology would remain intact and cancerous margins could still be recognizable both grossly and through microanalysis. To test this in the future, we will place cancerous tissue into gels that reach increasingly higher temperatures during setting and then we will process, stain, and analysis the tissue to determine whether the cancerous morphology can be recognized through any potential thermal damage that occurs to the surface cell layers. If we are able to show that temperature is not a limitation, then we will be able to use significantly faster setting gels (<3 minutes) to further minimize time spent in the operating room.

IV. X-RAY ABSORBANCE OF DEVICE HARDWARE AND GEL

Intraoperative radiography of excised breast tumor specimens is a standard practice for evaluating tumor inclusion (McCormick, 2004). Therefore, it is necessary that any device used in this process not interfere with the physician's ability to identify cancerous lesions.

We identified 12 target gel formulations of varying properties and prepared them in order to examine the x-ray absorbance of each gel. We prepared and cut the gels into wedges and placed them onto a Siemens Inveon MicroCT with the image acquisition parameters provided in Figure IV.1(A). The MicroCT was calibrated to Hounsfield units (HU) using water samples that yielded an expected value of 1 HU. We then used Inveon Research Workplace software to reconstruct the image using the parameters in Figure IV.1(B). The final reconstructed image is shown in Figure IV.2 below.

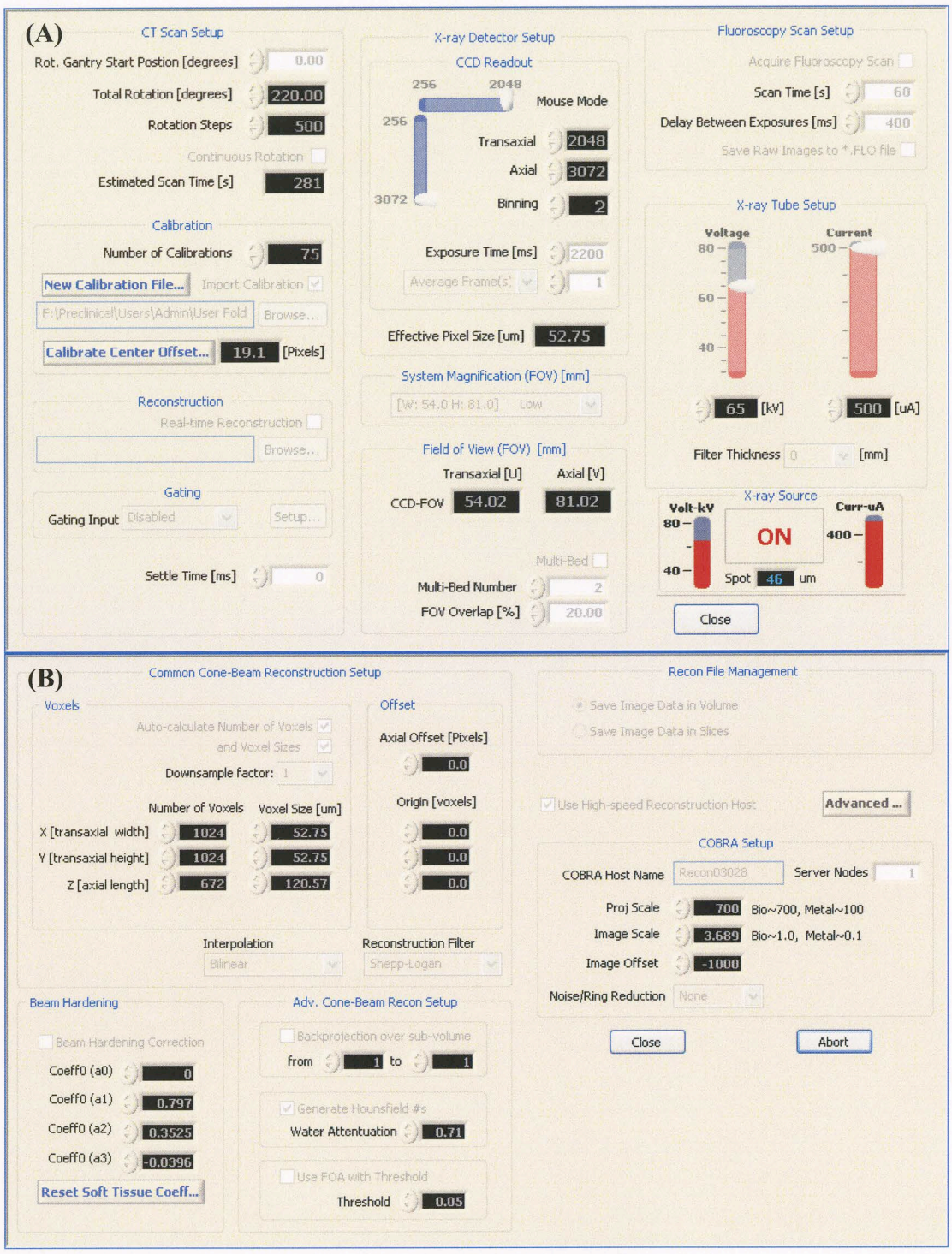

Figure IV.1. Screenshots of (A) image acquisition protocol used to obtain all MicroCT images and (B) the parameters used to reconstruct the MicroCT images.

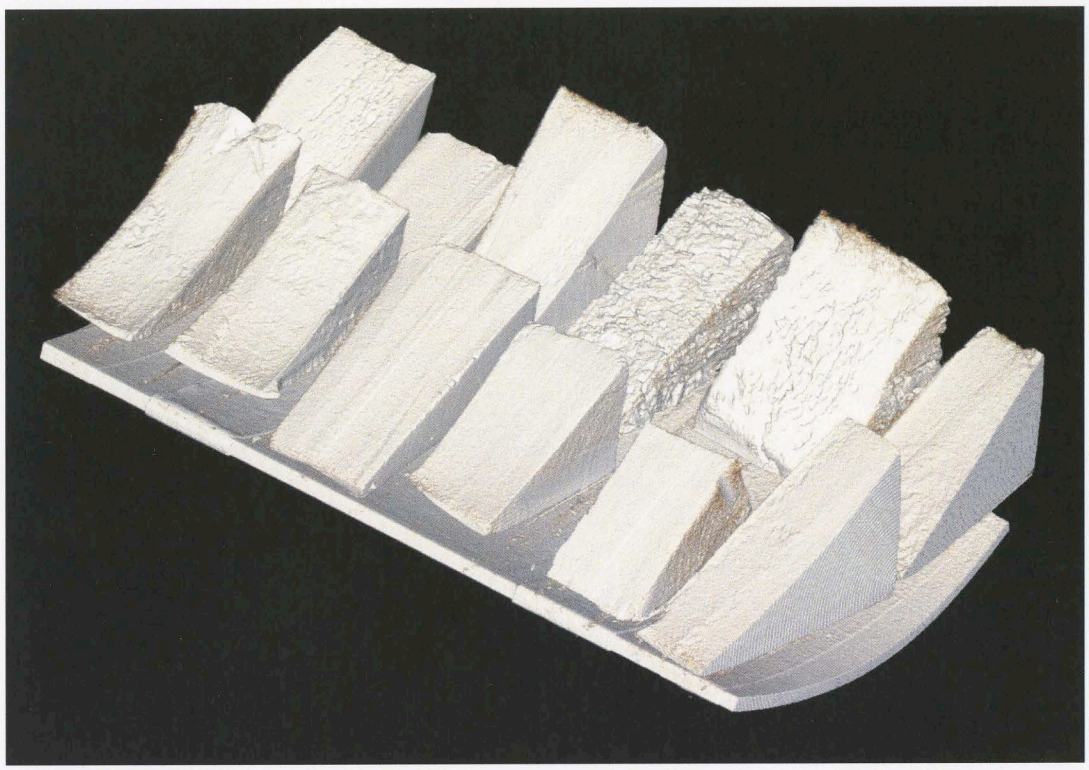

Figure IV.2. The reconstructed MicroCT image of the gels using 3D Visualization software by Visage.

We selected a spherical Region of Interest (ROI) with a volume of 72.9 mm^3 in which the voxel values were shown in Houndsfield units (HU); the HU values for each voxel within the ROI was averaged and recorded. Figure IV.3 illustrates the process of selecting an ROI within each sample. The resulting averaged HU values are presented in Table III.1.

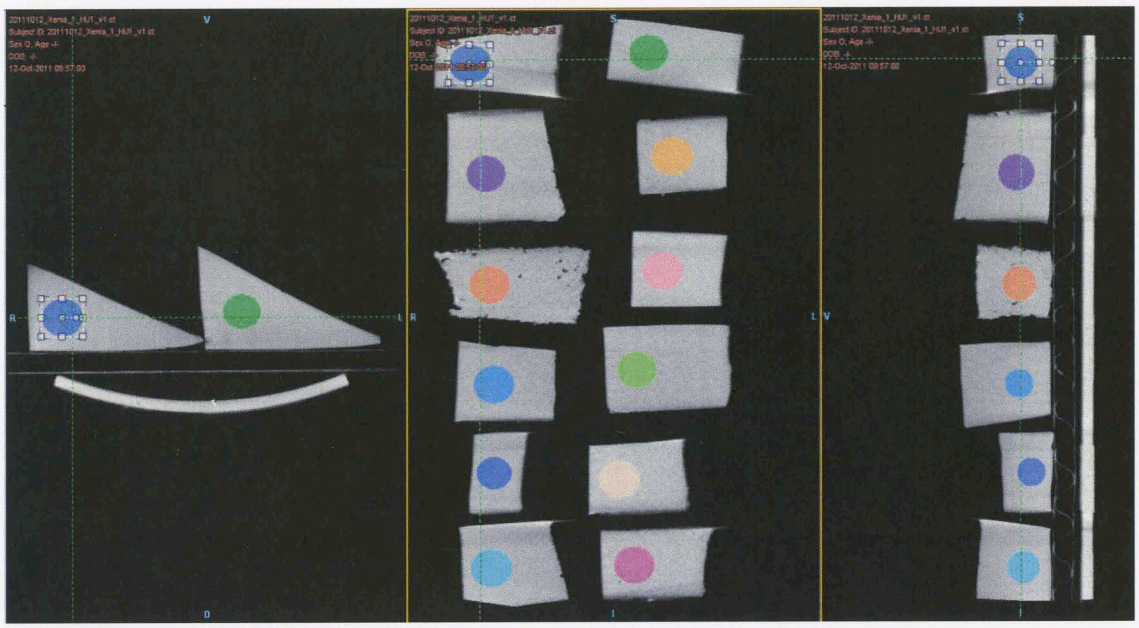

Figure IV.3. Screenshot of the process of selecting the spherical ROI and positioning it within each gel sample using the three-dimensional view provided by Inveon Research Workplace software.

Table IV.1. Averaged Hounsfield unit values for each imaged gel.

Gel #	HU
4	153.4
19	146.2
20	161.5
8	105.2
16	105.2
17	123.2
5	184.3
13	117.4
26	190.4

6	119.5
7	132.3
10	121.3

The HU values for the group of gels range from approximately 105-190 HU, a range close to that of soft tissues (GE Heathcare, 2011). Due to the narrow range between the gels and the similarity to the values of tissue, any of the formulations may be used in the device based on only this property.

Given that the hardware will be radiographed along with the gel, it was important to collect x-ray absorption data for potential plastics that will be used in the device. We collected a set of samples from a local Tucson rapid prototyping facility then scanned the group of samples with the same parameters as the gels above. The reconstructed image is shown in Figure IV.4.

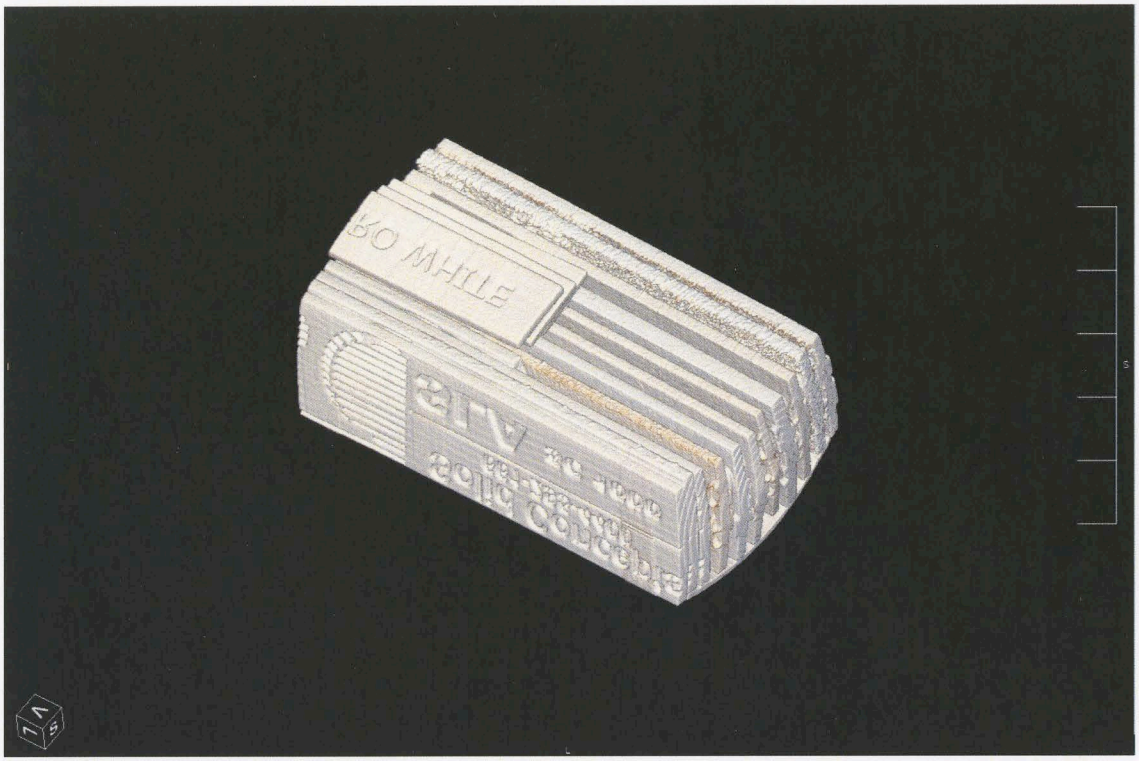

Figure IV.4. The reconstructed MicroCT image of the plastic samples using 3D Visualization software by Visage.

For analysis of the x-ray absorbance of the plastic samples, we selected a cubic ROI of a volume 50.1 mm^3, as illustrated in Figure IV.5. The averaged voxel values in HU are presented in Table IV.2.

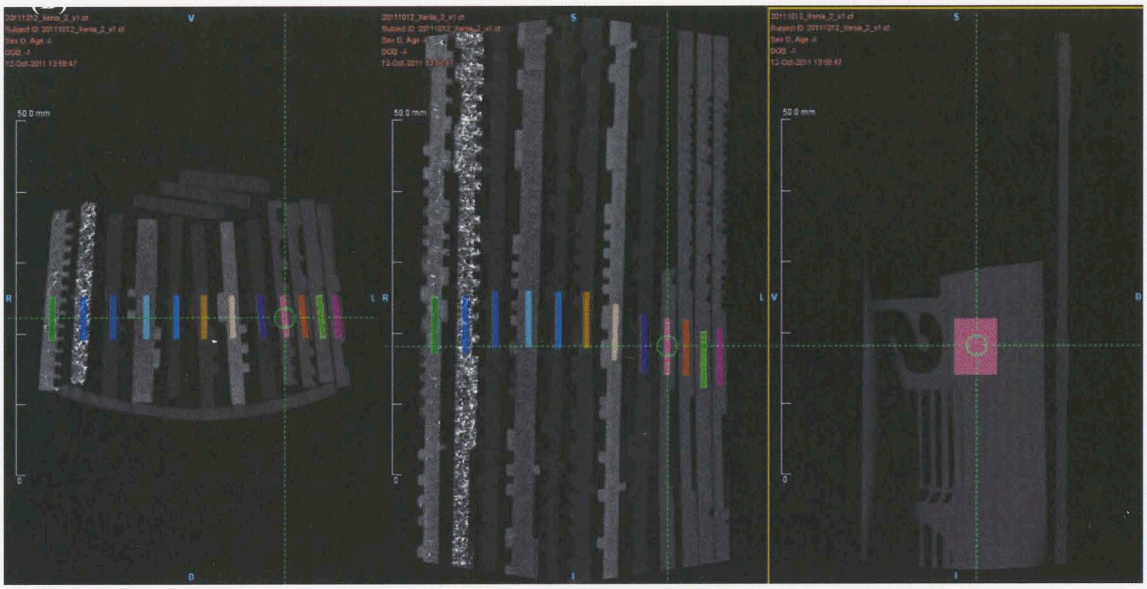

Figure IV.5. Hardware sample plastics MicroCT reconstruction in (A) 3D Visualization and (B) Inveon Research Workplace with selected the ROIs highlighted.

Table IV.2. Averaged Hounsfield unit values for each imaged plastic sample.

Plastic characterization	HU
LS Duraform HST	932.4
SLS FR-106	1271.5
SLS NyTek 1200 CF	-183.2
SLS Nylon 12 AF	443.9
SLS NyTek 1100	-192.2
SLS NyTek 1100 B	-36.2
SLS Nylon 12 GF	782.7
SLS Nylon 12	-235.7

SLA /Half	298.8
SLA Accura 50	358.2
SLA SC 4500	399.1
SLA SC 1000	344.7
Vero White	-38
Clear	-76.5
Vero Blue	-1.9

The HU values of the various plastics vary significantly, covering spectrums from gases to soft tissue to cancellous bone (GE Heathcare, 2011). This data is useful in determining which plastics will be suitable for the device. Generally, as x-ray absorbance decreases, likelihood of signal interference is reduced, making materials better suited for our application; SLS NyTek 1200 CF, SLS NyTek 1100, and SLS Nylon 12, with values of less than 1 HU are of greatest interest for future testing with tissue.

As described previously, the HU values in Tables IV.1 and IV.2 were acquired for the purpose of assessing whether the device has the potential to interfere with the physician's ability to identify cancerous lesions. The most common method by which lesions are found using radiography is by identifying highly x-ray attenuating calcifications, a common feature of breast cancers (D'Orsi, 1991). Figure IV.6 below illustrates the HU ranges of the device gel and hardware in comparison to those of tissue and calcifications.

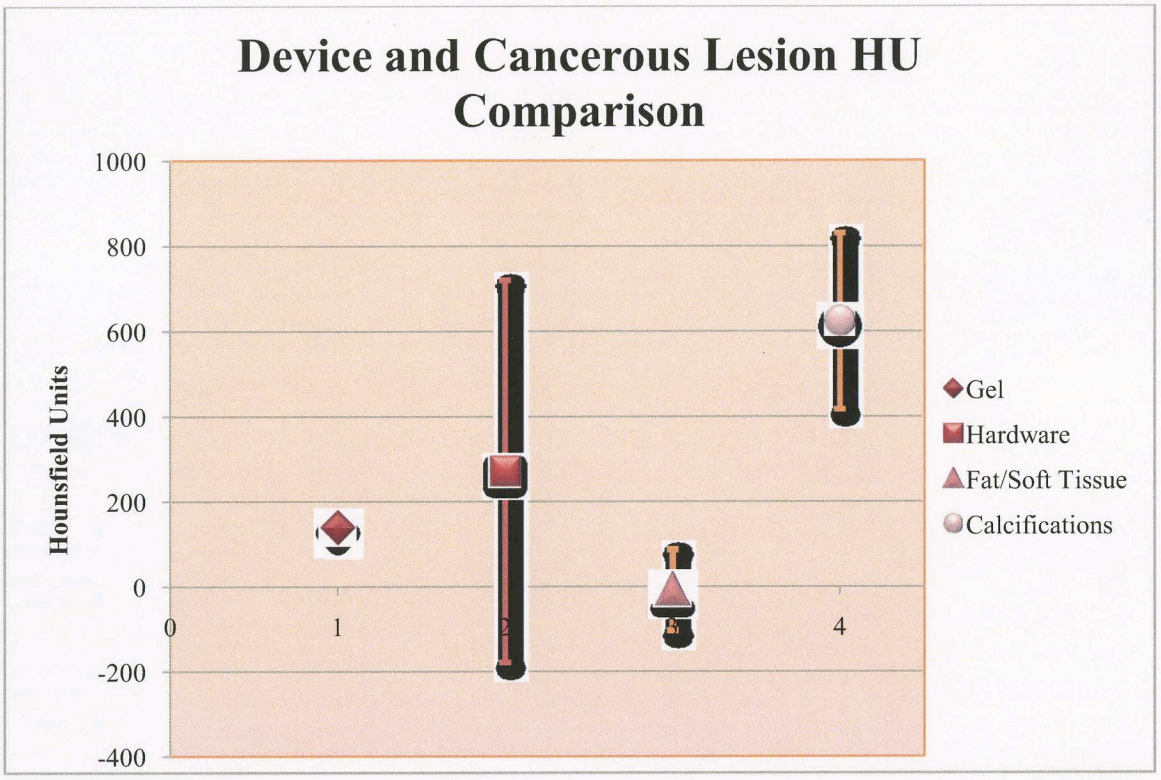

Figure IV.6. Comparison of the HU values of the gels and hardware with tissue and calcifications. Each point and its error bars are the average and standard deviation, respectively, of the values obtained.

The most important factor to note in this graph is the high HU values of the calcifications. If we couple any of the gels with plastics of radiodensity values of less than 1 HU, there is a significant gap between the device values and even the least x-ray absorbing calcifications. This supports the hypothesis that the device will very unlikely interfere with the assessment of cancerous lesions in the breast tissue using radiography.

V. PRELIMINARY TEST RESULTS ON CANINE TUMORS

One of the most important features to test with this device is any possible effect on down-stream tissue processes. If the gel interferes with the fixation, dehydration, paraffin penetration, or subsequent staining of the tissue, the results of margin assessment may be compromised. We designed a set of experiments to assess what, if any, effects the gel formulations have on these processes.

We acquired fresh samples of cancerous canine tumor tissue within 30 minutes of surgical excision. The tumor was approximately 5 cm^3 in volume, which we cut into 5 approximately equal sections, as illustrated in Figure V.1. One section was placed directly into a labeled 10% neutral buffered formalin container as a control and the remaining 4 sections were used for gel testing.

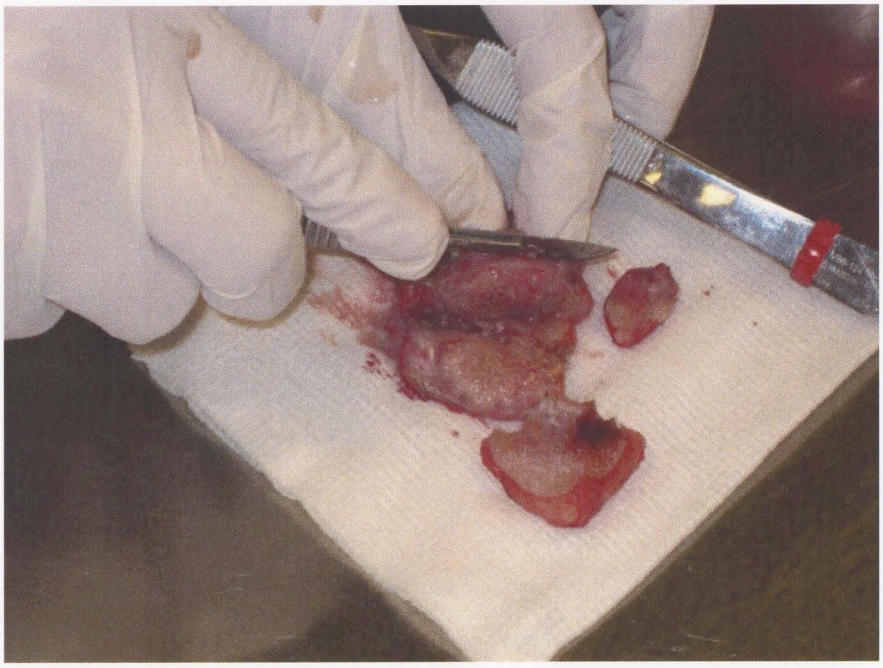

Figure V.1. Photograph of the canine tumor being sectioned by the veterinarian into 5 test samples.

We chose four gel formulations with the fastest setting times: #9, #16, #18, and #20 (components and respective quantities are presented in Table III.1) and prepared them ahead of time in the following manner; the PEGDE was mixed with water in a 100 mL plastic vial and the PEI was measured and kept in a separate vial, as shown in Figure V.2(A).

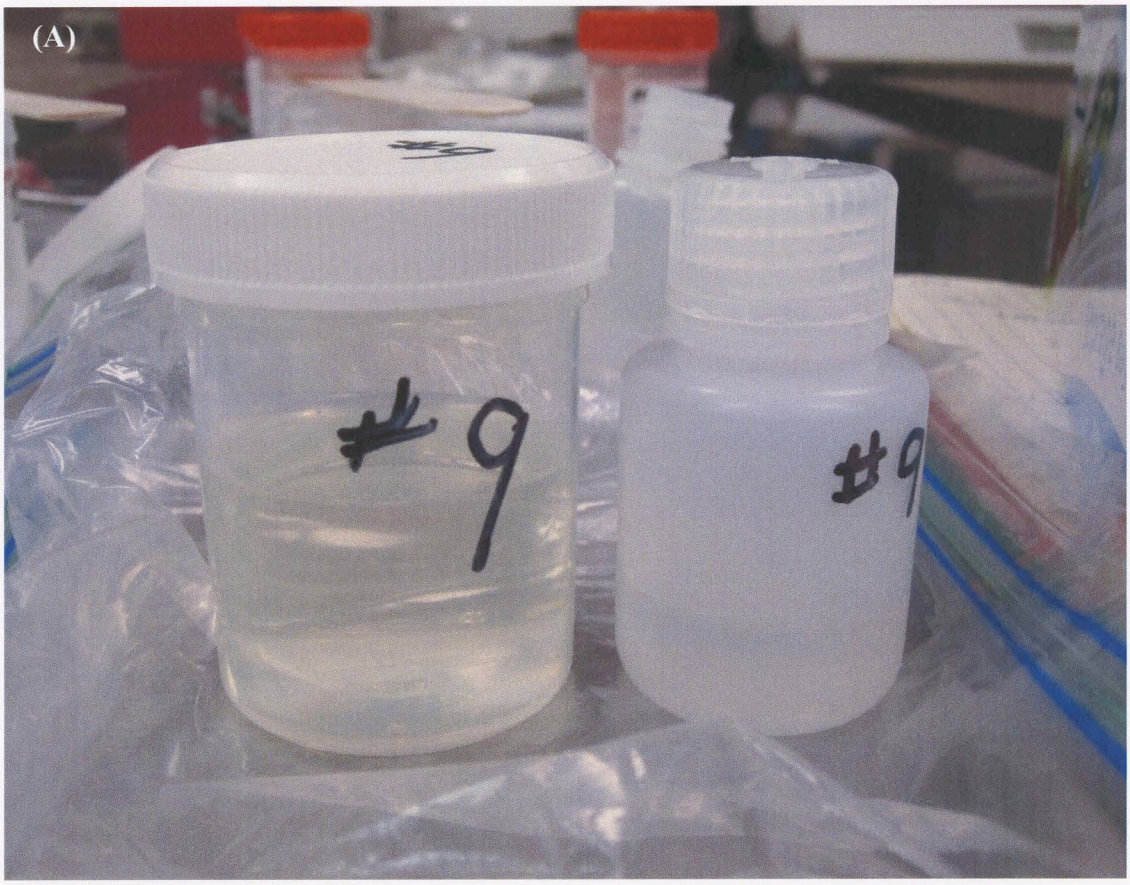

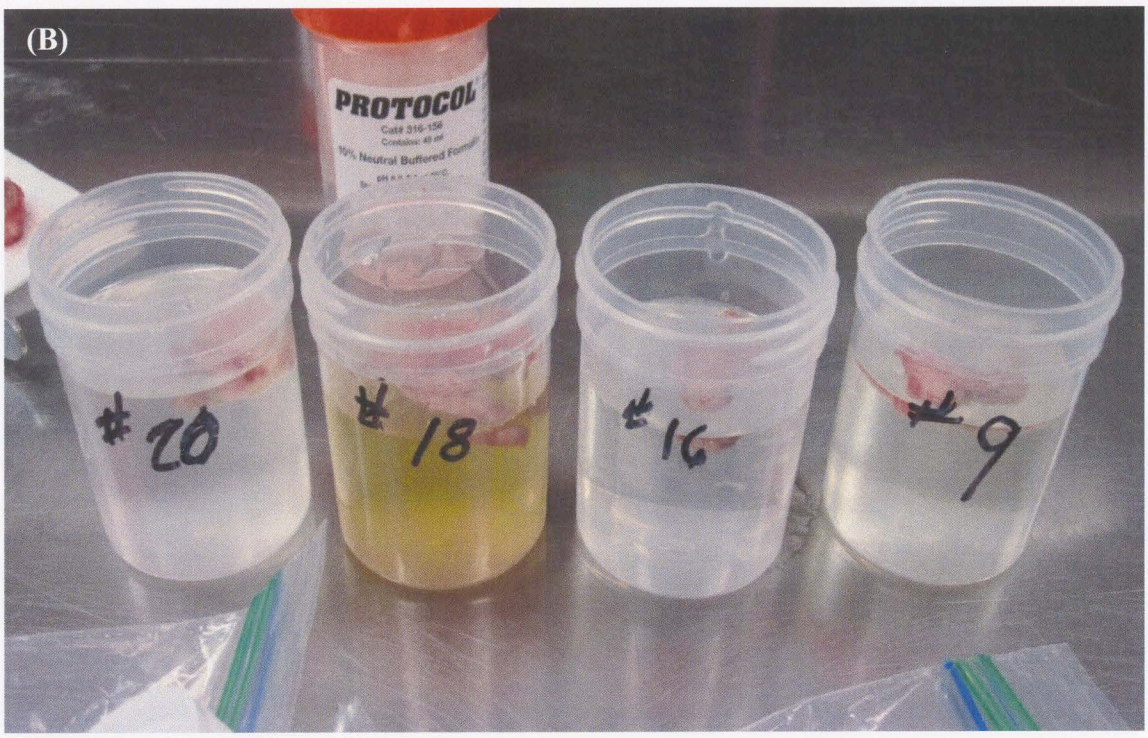

Figure V.2. (A) The right vial is the PEGDE which was added to the left vial containing PEI and water; (B) photograph of the tissue samples submerged in the 4 test gels during setting.

We poured the #9 PEI vial into the PEGDE/water vial and stirred together for approximately 30 seconds. We then submerged one of the tissue samples into the gel and waited for the formulation to set. Once setting was confirmed by prodding the gel surface, the tissue was cut from the gel and any surrounding gel was peeled from the tissue surface. The tissue sample was then placed into a 10% neutral buffered formalin container overnight. This was repeated for the remaining three formulations. Observations of the gels during setting were recorded and are presented in Table V.1 below.

Table V.1. Observations of gels containing tissue samples during and after setting.

Gel #	Comments
9	Set quickly (within 10 minutes), relatively easy to remove from the tissue sample after setting
16	Set quickly (within 10 minutes), relatively easy to remove from the tissue sample after setting
18	Very viscous and never set (after 5 hours of observation); tissue was removed and placed in formalin after 1.5 hours
20	Set within 10 minutes but consistency was very gooey and sticky, difficult to separate from tissue sample

After leaving in formalin overnight to ensure full fixation, all five samples were removed from their respective containers. Each tissue sample was placed into a tissue processing cassette and labeled with the gel formulation number or "Control" and the date.

The tissue cassettes were taken to the Arizona Vet Diagnostics Laboratory in Tucson, AZ and run through the standard tissue processing procedure (see Appendix). The samples were then hematoxylin and eosin stained and a veterinary pathologist with over ten years of experience assessed the following properties of the tissue slides, specifically comparing the control and the gel-encapsulated tissue samples: abruptness of keratinization, cell morphology and organization, chromatin patterns, basal membrane

and dermal collagen appearance, and the distinction between basophilic and eosinophilic areas. The resulting tissue images are shown in Figure V.3 below.

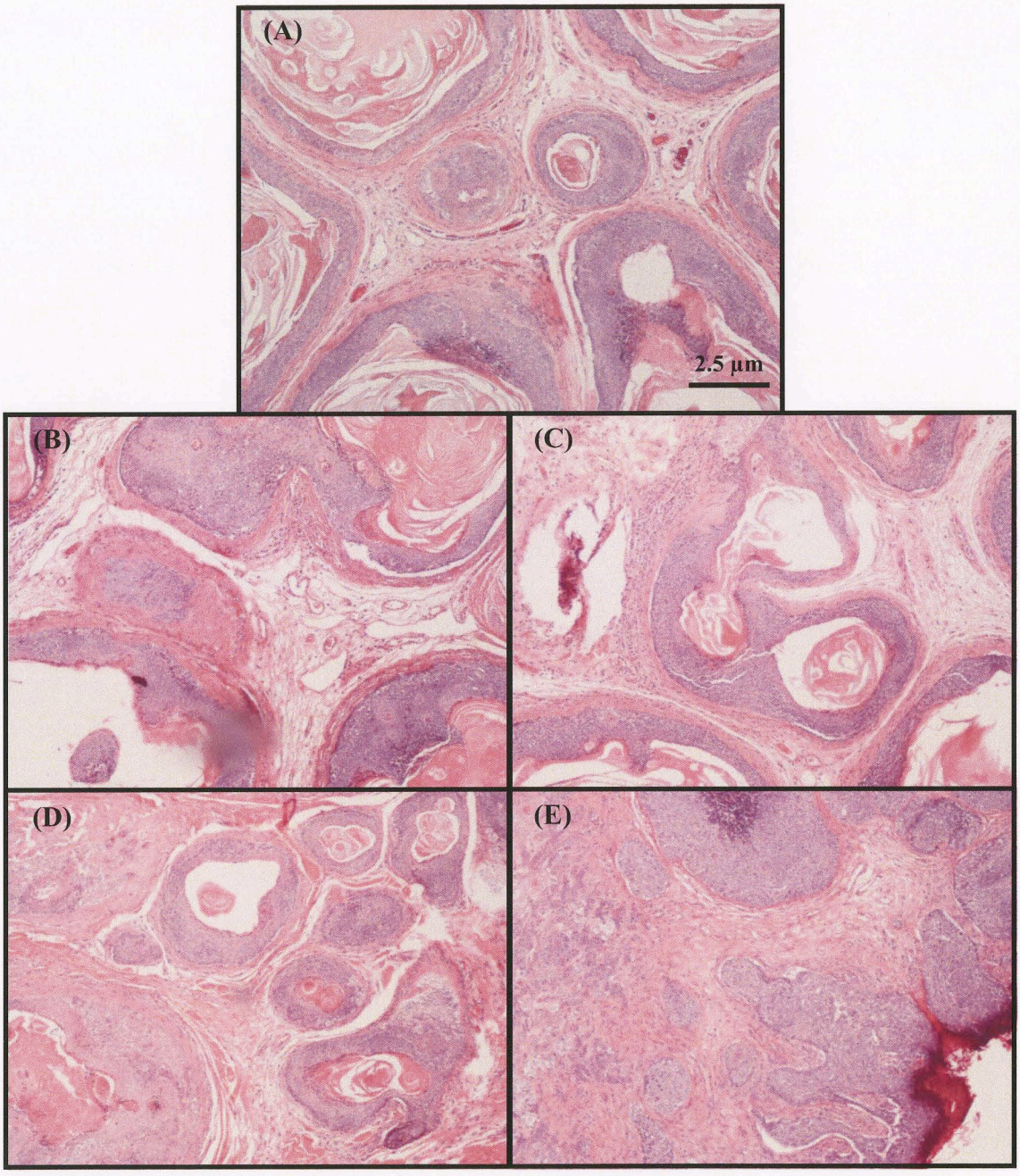

Figure V.3. Images of canine cancerous tissues following processing and staining; (A) control and gels (B) #19, (C) #20, (D) #16, and (E) #18.

The pathologist, Dr. Sharon Dial of the Arizona Veterinary Diagnostic Laboratory, determined that the stained tissue properties of the gel-encapsulated samples appear indistinguishable from the control sample. This confirms that the gel formulations have no effect on tissue properties and therefore may be used in clinical applications.

VI. CONCLUSIONS AND FUTURE WORK

The overall purpose of the studies described in this document was to find a starting point for clinical testing of the device. In order to accomplish this, it was necessary to design the device in a manner that addresses all fundamental limitations of current practices as well as to test the gel component for any potential interference with tissue properties.

We designed a hardware component that addresses the needs for accurate orientation of excised breast cancer tissue specimens. We were able to narrow down our pre-determined list of gels based on a limited allowance for setting time in the operating room and the maximum thermal threshold of tissues. Gels of interest set between 5-10 minutes and reach a maximum temperature of under 54°C. Since the setting times of the gels are dependent on several variables including volume of the formulation and order of component mixing, it is necessary to do further testing on the various formulations at different volumes. For initial clinical testing, however, we will be aim to work with tumor specimens of ~2 cm in diameter therefore the gels setting in under 10 minutes in Figure III.1(A) are of greatest interest.

Our MicroCT data confirmed that the x-ray absorptive properties of the gel are similar to that of tissues, highly minimizing any chance of artifacts that may inhibit a physician's ability to identify a lesion on a radiograph.

Obtaining tissue data was a cornerstone in this research. Confirmation that the gel does not in any way affect the tissue processing, staining, and microscopic analysis of

tumor tissue successfully addresses the fundamental question as to whether it may be used in a clinical setting at all.

The next stage of this project is the preparation for clinical studies. Following setting time, a major purpose of the gel is to provide support for tissue sectioning. The way in which we will determine the best gel for this is by making the ten most promising formulations with tissue and allowing a random sampling of pathologists to slice each and determine the one of greatest interest. Additionally, we will test the sliceability of the gels for sectioning on a microtome, a step in the microanalysis of tumor margins. Similar to the OCT compound described in "Current Tools" (p. 28), the device gel polymers may have the potential to penetrate tissue in a manner that eliminates the need to embed the samples in paraffin, a process that takes hours to complete. This property will be tested by placing thin (5 mm) tissue sections into the gel in a specimen block then assessing whether the microtome was able to cut through the gel and tissue block in a manner that facilitates microscopic examination of slides.

Once we have isolated the most promising formulations, we will make a rapid prototype from the mechanical drawings. Due to the volume of samples available through our veterinary partners, we will conduct our first clinical study using canine cancerous tissue. The goal is to show significant improvement in margin analysis by assessing changes in number of repeat surgeries as well as the long-term incidence of local recurrence. Additionally, we will collect information regarding the usefulness of the hardware markings, ease of gel and tissue slicing, total assessment time, and any unforeseen complications associated with device use.

Meanwhile, it is important to understand more of the specific properties of the gel formulations and what variables affect characteristics such as set time, temperature, ductility, and paraffin penetration. We will design a study to examine the effect of polymer chain lengths and the ratio of the three gel components on each of these characteristics.

In developing this technology and describing it to physicians, we discovered that it has applications in other surgical cancer types. Specifically, these cancer types, listed in Table VI.1, use the same tissue sectioning process for margin assessment either intra- or post-operatively. Once we optimize the device for applications in breast cancer, we will begin developing devices for other indications, taking into account size and orientation specifications.

Table VI.1. A list of cancers, the average size of the target organ, and any known considerations for device design.

Disease	Avg. Organ Volume (cm^3)	Considerations
Breast	560	Higher adipose content therefore longer fixation necessary
Prostate	60	Sectioning only for radical prostatectomy
Melanoma of skin	3	Intra-operative preferred but frozen sectioning distorts cells
Thyroid	10	Partial resections common
Lung	6000	For lobectomies, margins are performed intra-operatively
Kidney	216	If partial nephrectomy, intra-operative margins are evaluated
Corpus uteri	94	Necessary to evaluate depth of invasion of tumor
Pancreas	5	
Oral cavity & pharynx	300	Large variations in volume possible
Liver	3900	Partial resection is common
Ovary	9	
Testis	20	
Bladder	600	Pre-sectioning expansion of organ necessary

Through the studies presented in this document, we have shown a unique and useful solution to address the need for standardized gross pathology assessment in breast cancer treatment. We believe that the implementation of our device will result in significantly improved statistics of repeat surgery incidence and local recurrence rate and, as a result, will make breast-conserving surgery a viable and desirable option for hundreds of thousands of women worldwide.

APPENDIX

Tissue Processing Protocol

NORMAL OVERNIGHT

PROGRAM SCT

Station No.	Solution	Code No.	Conc.	Time (hr:min)	Set Temp.	P/V	Mix
1	FORMALIN		10 %	45 MIN		ON	SLOW
2	FORMALIN		10 %	45 MIN			
3	70 % ALC		70 %	45 MIN			
4	80 % ALC		80 %	45 MIN			
5	95 % ALC		95 %	45 MIN			
6	95 % ALC		95 %	1 HR			
7	100 % ALC		100 %	45 MIN			
8	100 % ALC		100 %	1 HR			
9	XYLENE		100 %	45 MIN			
10	XYLENE		100 %	1 HR			
11	PARAFFIN			35 MIN	58°		
12	↓			35 MIN	↓		
13				35 MIN			
14	↓			35 MIN	↓	↓	↓

REFERENCES

Smart-Surgery. (2011). Retrieved Dec 2, 2011, from Clinical Tutorials: http://smart-surgery.tripod.com/id16.html.

Abe, H., Hiroyuki, N., et al. (2000). Occult Breast Cancer Presenting Axillary Nodal Metastasis: A Case Report. Japanese Journal of Clinical Oncology, 14: 185-187.

Alexander, H. Hapfelmeier, A., & Elter, M. (2011). Needs assessment for next generation computer-aided mammography reference image databases and evaluation studies. International Journal of Computer Assisted Radiology and Surgery, 6: 749-767.

American Cancer Society. (2011, Sept 29). Breast Cancer. Retrieved Oct 5, 2011, from American Cancer Society: http://www.cancer.org/Cancer/BreastCancer/DetailedGuide/breast-cancer-what-is-breast-cancer.

American Chemical Society. (2011). Chemistry Review: Chemical Change. Retrieved Dec 2, 2011, from http://www.inquiryinaction.org/chemistryreview/chemical_change/.

Antoniotti, S., Antonczak, S., & Golebiowski, J. (2004). Acid-catalysed oxidative ring-opening of epoxide by DMSO. Theoretical investigation of the effect of acid catalysts and substituents. Theor Chem Acc, 112: 290–29.

Atkins, J.L. et al. (1972). Treatment of early breast cancer: a report after ten years of a clinical trial. Br Med J, 2: 423-429.

Baeyens, K., Jancarik, J., et al. (1994). Use of low-molecular-weight polyethylene glycol in the crystallization of RNA oligomers, 50: 764-767.

Banister, M., Vohnout, S., et al. (2007). Development of a PACS Digital Pump™ and Implications for other Industries. Proceedings of the SPIE - The International Society for Optical Engineering, 65270N-65279N.

Bankfalvi, A., Boecker, W., et al. (2004). Comparison of automated and manual determination of HER2 status in breast cancer for diagnostic use: A comparative methodological study using the Ventana BenchMark automated staining system and manual tests. International Journal of Oncology, 25: 929-935.

Baron, L. F., Baron, P.L., et al. (2000). Sonographically Guided Clip Placement Facilitates Localization of Breast Cancer After Neoadjuvant Chemotherapy. Amer. J. of Roentgenology, 174: 539-540.

Brown, J. B. (2010). Optical Assesssment of Tumor Resection Margins in the Breast. IEEE Journal of Selected Topics in Quantum Electronics, 16: 530-544.

Cesar, W. C., Chan, J., et al. (2007). The contribution of bifunctional SkipDewax pretreatment solution, rabbit monoclonal antibodies, and polymer detection systems in immunohistochemistry. Archives of Pathology & Laboratory Medicine, 131: 1047-1055.

Croshaw, R., Kim, Y., et al. (2011). Avoiding Mastectomy: Accelerated Partial Breast Irradiation for Breast Cancer Patients with Pacemakers or Defibrillators. Annals of Surgical Oncology, 18: 3500-3505.

D'Orsi, C. (1991). Early detection of breast cancer: Mammography. Breast Cancer Research and Treatment, 18: S107-S109.

Dewhirst, M., Viglianti B.L., et al. (2003). Basic principles of thermal dosimetry and thermal thresholds for tissue. International Journal of Hyperthermia, 19: 267–294.

Deyanira, S., Renato, N., et al. (2009). Comparison of the effect of cryopreservation protocols on the histology of bioengineered tissues. Histology and Histopathology, 24: 1531-1540.

Dooley, W., Parker, J. (2005). Understanding the mechanisms creating false positive lumpectomy margins. American Journal of Surgery, 190: 606-608.

Dorrius, M., der Weide, M.C., et al. (2011). Computer-aided detection in breast MRI: a systematic review and meta-analysis. European Radiology, 21: 1600-1608.

Feldman, S., Ibarra, J., et al. (2005). Policy Statement on Routine Orientation of Excised Breast Specimens. Am Soc Breast Diseases.

Felix, D., Ulrich, B. (2011). Breast Tomosynthesis. Seminars in Ultrasound CT and MR, 32: 281-287.

Fisher, B., Anderson, S. et al. (1995). Reanalysis and results after 12 years of follow-up in a randomized clinical trial comparing total mastectomy with lumpectomy with or without irradiation in the treatment of breast cancer. N Engl J Med, 333:1456-61.

Fisher, B., Anderson, S. et al. (2002). Twenty-Year Follow-up of a Randomized Trial Comparing Total Mastectomy, Lumpectomy, and Lumpectomy plus Irradiation for the Treatment of Invasive Breast Cancer. N Engl J Med, 347: 1233-1241.

Fisher, B., Bauer, M., et al. (1985). Five-year results of a randomized clinical trial comparing total mastectomy and segmental mastectomy with or without radiation in the treatment of breast cancer. N Engl J Med, 312: 665-73.

GE Heathcare. (2011, October 14). Hounsfield Unit. Retrieved from Medcyclopaedia: http://www.medcyclopaedia.com/library/topics/volume_iii_1/h/hounsfield_unit.aspx.

Geisbert, T. et al. (2010). Postexposure protection of non-human primates against a lethal Ebola virus challenge with RNA interference: a proof-of-concept study. The Lancet, 1896-1905.

Gene Research Lab. (n.d.). Retrieved Nov 30, 2011, from Tissue-Tech O.C.T. Compound : http://www.gene-rl.com/pdf/Tissue-Tech%20OCT.pdf

Goyal, R. Bansal, R., et al. (2011). 1,4-Butanediol diglycidyl ether (BDE)-crosslinked PEI-g-imidazole nanoparticles as nucleic acid-carriers in vitro and in vivo. Molecular Biosystems, 7: 2055-2065.

Gu, Q., David, F., et al. (2011). Evaluation of ionic liquid stationary phases for one dimensional gas chromatography-mass spectrometry and comprehensive two dimensional gas chromatographic analyses of fatty acids in marine biota. Journal of Chromatography, 1218: 3056-3063.

Guenther, J., Kirgan, D., et al. (1996). Feasibility of Breast-Conserving Therapy for Younger Women With Breast Cancer. Arch Surg., 131:632-636.

Hitchman, R., Murguía-Meca, F., et al. (2011). Baculovirus as vectors for human cells and applications in organ transplantation. Journal of Invertebrate Pathology, 107: S49-S58.

Hughes, D. J. (2008). Use of association studies to define genetic modifiers of breast cancer risk in BRCA1 and BRCA2 mutation carriers . Fam Cancer, 7: 233-244.

Ishida, M., Doi, K., et al. (1996). Digital image processing: Effect on detectability of simulated low-contrast radiographic patterns. Radiology, 201:745.

Jean-Philippe, Dreier, B. et al. (2010). Designed ankyrin repeat proteins: a novel tool for testing epidermal growth factor receptor 2 expression in breast cancer. Modern Pathology, 23: 1289-1297.

Karssemeijer, N. Frieling, .T, & Hendriks, J. (1993). Spatial resolution in digital mammography. Invest Radiol., 28: 413-419.

Kausik, M, Panda, A.K. (2011). Physicochemical Studies on the Interfacial and Micellization Behavior of CTAB in Aqueous Polyethylene Glycol Media. J. of Surfactants and Detergents, 14: 563-576.

Kearney, T, Morrow, M. (1995). Effect of Reexcision on the Success of Breast-Conserving Surgery. Annals of Surgical Oncology, 2: 303-307.

Keller, M., Majumder, S., et al. (2010). Autofluorescence and Diffuse Reflectance Spectroscopy and Spectral Imaging for Breast Surgical Margin Analysis. Lasers in Surgery and Medicine, 42: 15-23.

Kennedy, S, Geradts, J., et al. (2010). Optical breast cancer margin assessment: an observational study of the effects of tissue heterogeneity on optical contrast. Breast Cancer Research, 12: R91.

Kleinberg, D., Wood, T., et al. (2009). Growth Hormone and Insulin-Like Growth Factor-I in the Transition from Normal Mammary Development to Preneoplastic Mammary Lesions. Endocrine Reviews, 30: 51-74.

Kreppel, F., Kochanek, S. (2007). Modification of Adenovirus Gene Transfer Vectors With Synthetic Polymers: A Scientific Review and Technical Guide. Molecular Therapy, 16: 16–29.

Kumar, M. Majumdar, T., & Mahapatra, A. (2011). Kinetics of the basic hydrolysis of tris(1,10-phenenthroline)Fe(II): Influence of polymer-surfactant interactions. Colloids and Surfaces A: Physicochemical and Engineering Aspects, 380: 300-307.

Kurbet, S., de Barros, A., et al. (2006). The safe association of intraoperative evaluation of surgical margins and neoadjuvant chemotherapy in breast cancer larger than 3 centimeters. Breast J., 92: 28-36.

Lee, K., Kim, K., et al. (2001). Studies on a new series of cross-linked polymer electrolytes for a lithium secondary battery. J. Electrochem. Soc., 148: A1148-A1152.

Li, Y., Gao., B., et al. (2011). Studies on Preparation and Recognition Characteristic of Surface-Ion Imprinting Material IIP-PEI/SiO2 of Chromate Anion. Separation Science and Technology, 46: 1472-1481.

Macario, A. (2010). What does one minute of operating room time cost? Journal of Clinical Anesthesia, 22: 233–236.

Mahadevan-Jansen, A. Keller, M., et al. (2011). Looking Below the Surface of Breast Tissue During Surgery. Spectroscopy, Supplement: 48-58.

Marazzi, P. (n.d.). Science Photo Library. Retrieved Dec 2, 2011, from Breast cancer, X-ray image: http://www.sciencephoto.com/media/252263/enlarge.

Mayo Clinic. (2011). Mayo Clinic. Retrieved Nov 9, 2011, from Breast calcifications: http://www.mayoclinic.com/health/breast-calcifications/MY00101/DSECTION=causes.

McCormick, J., Keleher, A., et al. (2004). Analysis of the use of specimen mammography in breast conservation therapy. Am J of Surg, 188: 433-436.

Mercer University School of Medicine. (2011). Internet Pathology Laboratory for Medical Education. Retrieved Nov 11, 2011, from Histotechniques: http://library.med.utah.edu/WebPath/HISTHTML/HISTOTCH/HISTOTCH.html

Michigan State University. (n.d.). Chemical Reactivity. Retrieved Dec 2, 2011, from http://www2.chemistry.msu.edu/faculty/reusch/VirtTxtJml/react1.htm.

Moghimi, S., Symonds, P., et al. (2005). A two-stage poly(ethylenimine)-mediated cytotoxicity: implications for gene transfer/therapy. Molecular Therapy, 11: 990-995.

Moritz, A, Henriques, F. (1947). The relative importance of time and surface temperature in the causation of cutaneous burns. Am J Pathol, 23: 695–720.

Oppenheimer, S. Mi, D., et al. (2010). Molecular Analysis of Tumor Margins by MALDI Mass Spectrometry in Renal Carcinoma. J. of Proteome Research, 9: 2182-2190.

Patel, H., Astley, S., et al. (2006). Automated breast tissue measurement of women at increased risk of breast cancer. Digital Mammography, Proceedings, 4046: 131-136.

Pinder, S. E. (2005, Jan). Pathology Reporting of Breast Disease. Retrieved Nov 11, 2011, from Approach to Cut-Up: Macroscopic Examination as the Precursor to Accurate Microscopic Interpretation - Breast: http://www.bdiap.org/Trainees2010/Pinder2010optimised.pdf.

Polysciences, Inc. (2007, Oct 10). Polysciences, Inc. Retrieved Oct 7, 2011, from Poly(ethylene glycol) Derivatives: http://www.polysciences.com/SiteData/poly/Assets/DataSheets/447.pdf.

ProtoMold. (2011). Design Guidelines: Simple, straight-pull parts. Retrieved Nov 16, 2011, from Protomold Injection Molding Service: http://www.protomold.com/DesignGuidelines_SimpleStraightPullParts.aspx.

Rossi, J.J. (2006). RNAi therapeutics: SNALPing siRNAs in vivo. Gene Therapy, 13: 583-584.

Rossouw, J. (2002). Risks and benefits of estrogen plus progestin in healthy postmenopausal women. Women's Health Initiative randomized controlled trial. JAMA, 288:321–333.

Rudolph, C., Lausier, J., et al. (2000). In vivo gene delivery to the lung using polyethylenimine and fractured polyamidoamine dendrimers. Journal of Gene Medicine, 2: 269–78.

Russo, I., Russo, J.. (2011). Pregnancy-Induced Changes in Breast Cancer Risk. Journal of Mammary Gland Biol Neoplasia, 16: 221–233.

Schmidt, M., Powers, K. (2011). Breast Imaging: Screening and Evaluation . Clin Obstet Gynecol., 54: 103-109.

Schmitz, A., van den Bosch, M., et al. (2010). Precise correlation between MRI and histopathology - Exploring treatment margins for MRI-guided localized breast cancer therapy. Radiother Oncol, 97; 225-232.

SEER. (2008). Age-Adjusted SEER Incidence Rates - Female Breast. Bethesda, MD: National Cancer Institutes of Health.

Shayan, K., Smith, C., et al. (2004). Reliability of intraoperative frozen sections in the management of Hirschsprung's disease. J Pediatr Surg, 39: 1345-1348.

Silverstein, M., Lagios, M., et al. (1999). The influence of margin width on local control of ductal carcinoma in situ of the breast. N Engl J, 340:1455-61.

Simpkins, J., Swenberg, J., et al. (2011). Atrazine and Breast Cancer: A Framework Assessment of the Toxicological and Epidemiological Evidence. Toxological Sciences, 123: 441-459.

Specht, K., Richter, T., et al. (2001). Quantitative Gene Expression Analysis in Microdissected Archival Formalin-Fixed and Paraffin-Embedded Tumor Tissue. American Journal of Pathology, 158: 419-429.

Stoll, A., Greene, L. (1959). Relationship between pain and tissue damage due to thermal radiation. J Appl Physiol, 14: 373–82.

Tangella, K. (2010). Tissue Pathology: A Clinical Perspective. In Nanobiophotonics (pp. 57-76). McGraw-Hill.

The Breast Care Site. (2011). TheBreastCareSite.com. Retrieved Nov 9, 2011, from *Why women choose a lumpectomy or a mastectomy*: http://www.amoena.com/tbcs/NewlyDiagnosed/BreastSurgeries/Mastectomy/Choosing+A+Lumpectomy+or+a+Mastectomy.htm.

Tzu-Chao, C. Hsu, S. et al. (2011). Magnolol down-regulates HER2 gene expression, leading to inhibition of HER2-mediated metastatic potential in ovarian cancer cells. Cancer Letters, 311: 11-19.

Uecker, J., Bui, E., et al. (2011). Intraoperative Assessment of Breast Cancer Specimens Decreases Cost and Number of Reoperations. American Surgeon, 77: 342-344.

University of Washington School of Medicine. (2012). Histology. Retrieved Nov 13, 2011, from Introduction to Tissue Fixation: http://histologycourse.com/Tissue%20Fixation-Lecture%2012.pdf.

Vancha, A., Govindaraju, S., et al. (2004). Use of polyethyleneimine polymer in cell culture as attachment factor and lipofection enhancer. BMC Biotechnology, 4: 23.

Vyborny, C. Giger, M., et al. (2000). Computer-aided detection and diagnosis of breast cancer. Radiologic Clinics of North America, 38: 725-740.

Walsh, A., Thompson, K., et al. (2010). Polyamine-Functional Sterically Stabilized Latexes for Covalently Cross-Linkable Colloidosomes. Langmuir, 26: 18039-18048.

Weidner, C. S. (2003). Modern Surgical Pathology. Philadelphia: Saunders.

Yamazoe, H., Tanabe, T. (2009). Cell micropatterning on an albumin-based substrate using an inkjet printing technique. J Biomed Mater Res A, 91: 1202-1209.

Yuan-Zhi, S. Liu, L., et al. (2011). Characterizing the Clustered Microcalcifications on Mammograms to Predict the Pathological Classification and Grading: A Mathematical Modeling Approach. Journal of Digital Imaging, 24: 764-771.

Zhao, Z., Wu, F. (2010). Minimally-invasive thermal ablation of early-stage breast cancer: A systemic review. EJSO, 36: 1149-1155.

Zopes, D. von Hagen, R., et al. (2010). Ink-jetable patterning of metal-catalysts for regioselective growth of nanowires. Nanoscale, 2: 2091-2095.